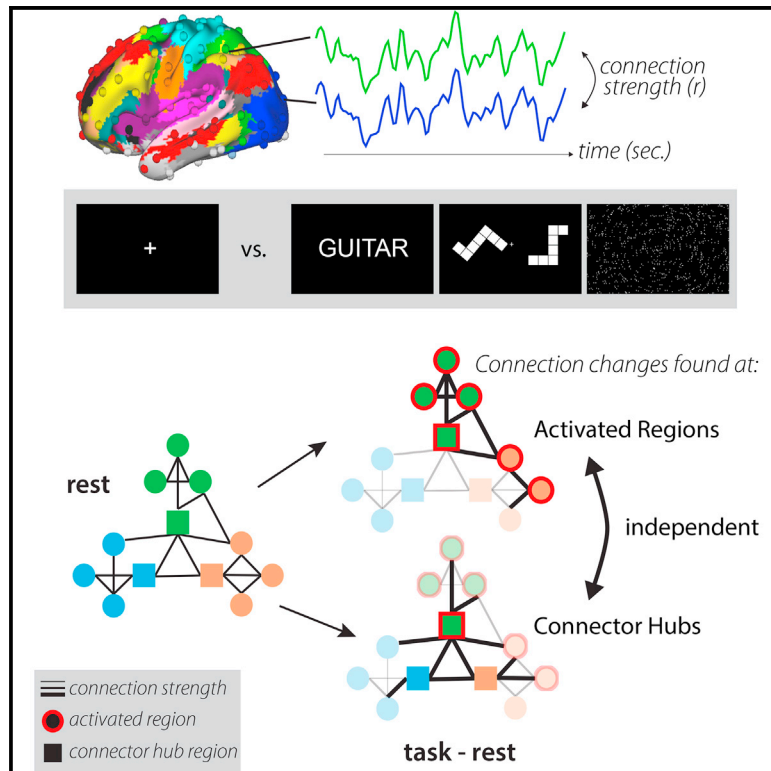


Cell Reports

Evidence for Two Independent Factors that Modify Brain Networks to Meet Task Goals

Graphical Abstract



Authors

Caterina Gratton, Timothy O. Laumann, Evan M. Gordon, Babatunde Adeyemo, Steven E. Petersen

Correspondence

cgratton@wustl.edu

In Brief

Gratton et al. show that, during tasks, human brain networks are subtly modified both at task-activated regions and at topologically important hubs. Classes of regions with these two properties show distinct patterns of network changes, suggesting they index dissociable factors for modifying brain networks in a task.

Highlights

- Human brain networks differ between rest and task at activated and hub regions
- Regions stratified by activation and hub-status show distinct FC-related attributes
- Activated hubs exhibit FC attributes consistent with enacting task control
- Findings suggest dissociable factors for linking brain regions in complex tasks



Evidence for Two Independent Factors that Modify Brain Networks to Meet Task Goals

Caterina Gratton,^{1,9,*} Timothy O. Laumann,¹ Evan M. Gordon,^{7,8} Babatunde Adeyemo,¹ and Steven E. Petersen^{1,2,3,4,5,6}

¹Department of Neurology

²Department of Radiology

³Department of Anatomy and Neurobiology

⁴Department of Biomedical Engineering

⁵Department of Psychology

⁶Department of Neurological Surgery

Washington University in St. Louis, St. Louis, MO 63110, USA

⁷VISN 17 Center of Excellence for Research on Returning War Veterans, Waco, TX 76711, USA

⁸Center for Vital Longevity, School of Behavioral and Brain Sciences, University of Texas at Dallas, Dallas, TX 75235, USA

⁹Lead Contact

*Correspondence: cgratton@wustl.edu

<http://dx.doi.org/10.1016/j.celrep.2016.10.002>

SUMMARY

Humans easily and flexibly complete a wide variety of tasks. To accomplish this feat, the brain appears to subtly adjust stable brain networks. Here, we investigate what regional factors underlie these modifications, asking whether networks are either altered at (1) regions activated by a given task or (2) hubs that interconnect different networks. We used fMRI “functional connectivity” (FC) to compare networks during rest and three distinct tasks requiring semantic judgments, mental rotation, and visual coherence. We found that network modifications during these tasks were independently associated with both regional activation and network hubs. Furthermore, active and hub regions were associated with distinct patterns of network modification (differing in their localization, topography of FC changes, and variability across tasks), with activated hubs exhibiting patterns consistent with task control. These findings indicate that task goals modify brain networks through two separate processes linked to local brain function and network hubs.

INTRODUCTION

Humans can easily and flexibly complete many different tasks depending on their goals. This ability depends on both specialized processing occurring in individual brain regions and coordinated interactions across distributed regions organized into large-scale networks (also called brain systems). A fundamental question of cognitive neuroscience is how specialized brain regions are able to flexibly link together to perform different tasks.

Using fMRI, functional networks can be identified even when individuals lie quietly without any explicit task in a “resting state,” based on patterns of correlated fMRI signal between brain

regions (i.e., functional connectivity [FC]) (Biswal et al., 1995; Power et al., 2011; Yeo et al., 2011). Recent studies have highlighted the consistent organization of functional networks at rest and during varied tasks (Betti et al., 2013; Cole et al., 2014; Krienen et al., 2014), suggesting that the brain’s large-scale networks are dominated by a fundamentally stable intrinsic backbone (Cole et al., 2014).

However, diverse behavioral states appear to be supported by smaller-scale changes that subtly modify brain networks (Cole et al., 2014; Krienen et al., 2014). Although the magnitude of these changes is small, it is possible to accurately decode the task state of a participant simply from their FC in a task (Alnæs et al., 2015; Gonzalez-Castillo et al., 2015; Shirer et al., 2012). In addition, task performance is related to these modifications of FC (Dwyer et al., 2014; Gonzalez-Castillo et al., 2015; Gordon et al., 2014; Hampson et al., 2010; Kelly et al., 2008), suggesting that the alterations are relevant to behavior.

Despite this evidence, previous studies have failed to provide an explanation for where and why network interactions vary during the engagement of a task. Here, we examine two hypotheses inspired by largely distinct literatures on localized and distributed processing (Figure 1): do networks change (1) because regions are activated in a task or, (2) because of inherent properties of the network’s organization?

The first possibility has motivated a host of studies examining functional connectivity changes among small sets of functionally “relevant” (or task-activated) regions. The logic is that regions specialized for individual cognitive operations are both simultaneously activated and need to interact to complete a complex task. For example, in visual attention tasks, changes in FC have been recorded between activated visual regions and activated attentional-control regions (Gazzaley et al., 2007; Spadone et al., 2015), presumably reflecting the need for control regions to communicate with visual regions. This view proposes that interactions among brain regions are altered in different contexts primarily due to the specialized functions of the individual brain regions.

An alternative view proposes that network interactions are guided by the topological structure of brain networks (Sporns,

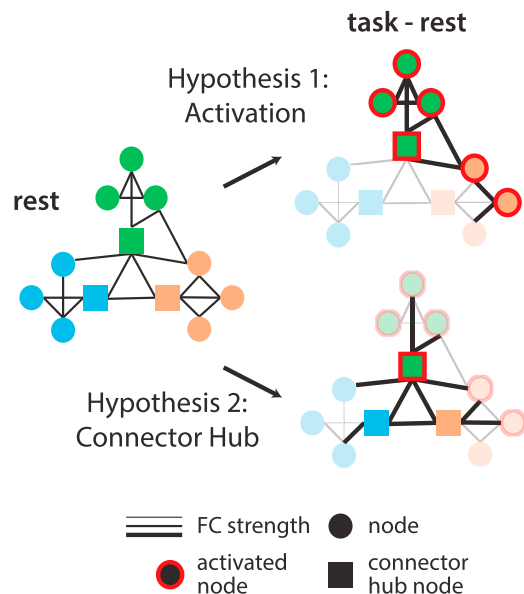


Figure 1. Proposed Factors Contributing to Task FC

Intrinsic network interactions (right) may be modified to accomplish task goals by changing connectivity between regions activated by a task (Hypothesis 1; activated regions shown with red outlines) or by changing connectivity patterns of specialized hub regions (Hypothesis 2; squares) that help connect networks to each other. Regions and connections without changes are faded in the right panel to emphasize differences.

2011). In this complex systems perspective, brain network properties are determined from the pattern of edges (here, FC) among nodes (brain regions), modeled as a graph, rather than by studying local processing characteristics of brain regions. In the brain graph, specialized connector hub locations are defined by having connections distributed across multiple different networks (Guimera and Amaral, 2005). These regions are seen as critical for coordinating interactions, and thereby information processing, across brain networks (Power et al., 2013). Therefore, strong changes in network interactions are predicted to occur at connector hubs. This view is supported by evidence that (1) brain lesions to connector hubs cause widespread disruptions in network organization (Gratton et al., 2012) and behavior (Warren et al., 2014), and (2) connector hubs in the frontoparietal network show malleable connectivity across tasks (Cole et al., 2013). These findings suggest a central role for connector hubs in network interactions but leave unclear how hubs relate to regional specializations in task control and processing.

We directly contrast these two hypotheses by using fMRI to measure functional brain networks in healthy participants at rest and engaged in three varied tasks. We examined activated and connector hub regions to determine which property most strongly associated with task-related FC alterations.

RESULTS

To examine how brain networks are altered during task and rest states, we analyzed fMRI data from 28 participants while they rested quietly or completed three tasks: a semantic task

requiring a noun/verb judgment on a presented word, a mental rotation task requiring a same/mirror image judgment on two objects, and a coherence task requiring a judgment of whether dots were arranged concentrically. These tasks are especially well-suited to our question, as they included varied stimuli (including verbal and non-verbal stimuli) and they call upon widely varying cognitive processes (e.g., language, mental manipulation, and perceptual grouping), with differing demands on task control and perceptual resources (Dubis et al., 2016) (e.g., varying in behavioral performance and activation of control systems). We measured functional brain networks in each state by computing correlations across 264 regions arranged into 13 systems (Figure 2A).

Network Organization Is Largely Similar during Task and Rest

To evaluate the overall effect of task state on FC network organization, we computed the similarity between task and rest by measuring the correlation between the connectivity matrices in each condition. On average, large-scale networks were very similar between task and rest (Figures 2B and 2C; “task” data is concatenated across all tasks). The correlation between task and rest group average FC matrices was $r = 0.95$ (Mantel’s statistic: $p < 0.001$; single subject matrices: $r = 0.73$, $SD = 0.04$). High correlations were also seen between rest and single tasks (semantic versus rest: $r = 0.94$; mental rotation versus rest: $r = 0.92$, coherence versus rest: $r = 0.94$, all $p < 0.001$; Figure S1A).

Furthermore, network topology was very similar during rest and task states. Data-driven assignment of regions to network communities was substantially unchanged by task engagement and was similar to previously published findings (Power et al., 2011) (quantified with normalized mutual information [NMI]: rest versus task $NMI = 0.80$; rest versus Power-2011 networks $NMI = 0.73$; task versus Power-2011 $NMI = 0.73$). In addition, we measured the similarity of connector hub locations across states, by calculating the participation coefficient (PC) metric (Guimera and Amaral, 2005) for each node. This metric measures the distribution of a region’s connections across different systems; regions with high PC are connector hubs. As with network organization, PC values during rest in our subjects were very similar to published findings from a large cohort (Power et al., 2013) ($r = 0.88$) and to PC during task ($r = 0.90$) suggesting that connector hub locations did not shift substantially during the performance of tasks. These findings indicate that the core intrinsic network organization is largely unchanged between rest and task states.

Subtle Systematic FC Differences Exist between Task and Rest

Despite the overall similarity in large-scale network structure, smaller-magnitude differences were present between task and rest. We measured differences by directly contrasting task and rest FC in a difference matrix (Figure 3A). Differences between the states were reliable: (1) p value distributions showed a significant enrichment of edges $p < 0.05$ compared with a permuted null distribution ($p < 0.001$), and (2) many individual connections remained significant after false discovery rate (FDR) correction (Figure S2).

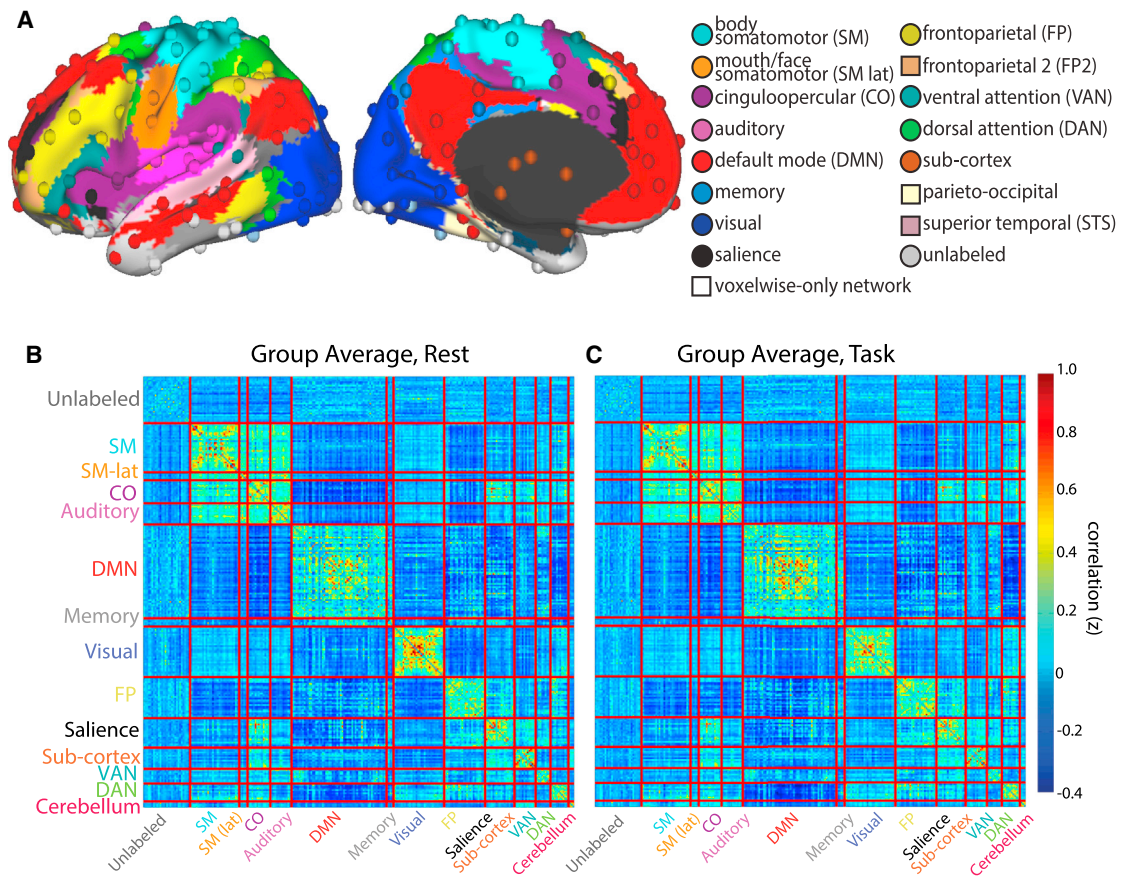


Figure 2. A Common FC Organization Is Present during Task and Rest States

(A) FC was calculated via time-series correlations among 264 cortical and subcortical regions of interest (spheres), distributed across 13 networks (Power et al., 2011) (sphere colors; surface colors represent networks used for voxelwise analyses).

(B and C) FC during rest (B) and task (C) is very similar, dominated by a strong network structure with high correlations within each system (diagonal) compared to between systems (off-diagonals; similar results were seen for individual tasks, see Figure S1A).

FC differences were observed both within and between networks. During tasks, within-network FC decreased within the visual system and, to a lesser extent, in other sensory systems (somatomotor [SM], lateral somatomotor [lat-SM], and auditory) as well as the subcortex. Increases in within-network FC during tasks were seen in the default mode (DMN) (Figure 3B, left). By contrast, between-network FC decreased in the DMN and increased for the visual system, as well as subsets of control systems (Figure 3B, right). These gross characteristics were consistent for single tasks (Figure S1B), despite their variable cognitive demands.

Activated Regions Alter FC, Primarily between Networks

Given the reliable changes in FC across participants and tasks, we asked whether changes were systematically related to the properties of individual regions. We examined two potential hypotheses (Figure 1): (1) FC is altered primarily for regions activated by a task, or (2) FC is altered primarily for connector hub regions that mediate interactions across different systems (see Figure S3 for activated and connector hub nodes).

To test the first hypothesis, we examined if FC was altered more in activated regions—that is, those exhibiting large absolute percent signal changes during the task—than non-activated regions. Note that FC was calculated after removing evoked activations from the task time series via regression to reduce spurious inflations of correlation measurements from co-activation as in Al-Aidroos et al. (2012) (see Figure S4 for activation results without task regression; as expected, these statistics were inflated compared with those reported below). We conducted a quartile analysis comparing the absolute changes in FC of regions, grouped based on their activation magnitude (top versus bottom 25%). We found that FC changed significantly more for activated than non-activated regions (compared with permutation testing here and in following tests: $p < 0.001$; individual tasks: all $p[\text{FDR}] < 0.01$ corrected across tasks, Figure S5A), providing evidence that the functional specialization of regions relates to their network modulations during tasks.

Next, we asked how activation-related changes in FC were distributed across within- or between-network connections. Compared with non-activated nodes, activated regions showed

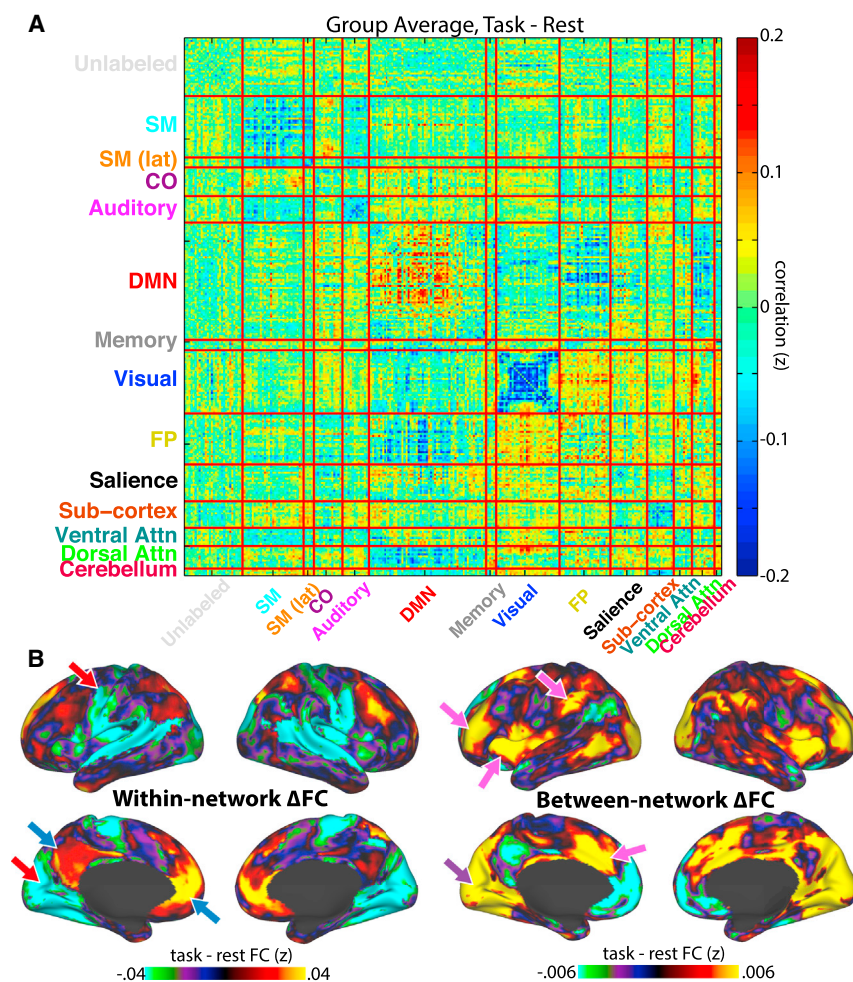


Figure 3. Subtle but Reliable FC Differences Were Present during Task and Rest States

Subtle but reliable differences were seen in the direct contrast of task and rest correlation matrices for 264 regions of interest (A) and on average for each voxel to other voxels within its own network (B, left) or voxels in other networks (B, right). FC changed within-system (along the diagonal, e.g., increases within the DMN, decreases within the visual and other sensory/motor systems; red and blue arrows in B) and between-systems (off-diagonal, e.g., increases between visual and subsets of control systems [e.g., CO, FP, DAN]; pink and purple arrows in B). These effects were consistent for individual tasks (Figure S1B).

change significantly more than non-connectors (bottom 25% of PC values) on average across the brain (permutation $p = n.s.$). Interestingly, however, significant differences were observed if between- and within-network FC changes were considered separately. Compared to non-connectors, connector hubs showed significantly increased modulation of between-network FC ($p < 0.001$), but significantly reduced modulation of within-network FC ($p < 0.001$; Figure 4, right). Individual tasks showed similar effects, with connector hubs exhibiting significantly higher between-system modulations in two of three tasks ($p[FDR] < 0.01$ for mental rotation and semantic tasks) and lower within-system FC in all three tasks (all $p[FDR] < 0.05$; Figures S5B and S5C). Thus, connector hubs ex-

hibited complex modulation upon entering task states, with a relative suppression of FC changes within a network, but enhanced changes in between network FC.

Again, results were robust to variations in analysis. We found similar relationships if the measures were treated as continuous variables: PC showed a positive correlation with between-network FC change (Figure S6, $\rho = 0.25$, $p < 0.001$) and a negative correlation with within-network FC changes ($\rho = -0.34$, $p < 0.001$, see also Table S1). Other binning thresholds produced similar results (Table S2). Adopting the Gordon et al. (2016) parcellation, using PC values computed from this dataset, or examining the PC of highest and lowest FC-change regions produced analogous results (all within- and between-network comparisons, $p < 0.01$). These findings support our second hypothesis, that FC changes during a task are related to connector hubs, but suggest that hubs differentially modulate different types of connections, showing relatively invariant connectivity within a system, while modulating connections between systems.

Hubs Show Complex FC Network Modulations

Our second hypothesis (Figure 1) proposes that task-related changes in FC will be seen at connector hubs. We found that the FC of connector hubs (top 25% of PC values) did not

change significantly more than non-connectors (bottom 25% of PC values) on average across the brain (permutation $p = n.s.$). Interestingly, however, significant differences were observed if between- and within-network FC changes were considered separately. Compared to non-connectors, connector hubs showed significantly increased modulation of between-network FC ($p < 0.001$), but significantly reduced modulation of within-network FC ($p < 0.001$; Figure 4, right). Individual tasks showed similar effects, with connector hubs exhibiting significantly higher between-system modulations in two of three tasks ($p[FDR] < 0.01$ for mental rotation and semantic tasks) and lower within-system FC in all three tasks (all $p[FDR] < 0.05$; Figures S5B and S5C). Thus, connector hubs ex-

hibited complex modulation upon entering task states, with a relative suppression of FC changes within a network, but enhanced changes in between network FC.

Activation and PC Are Separately Related to FC

A linear regression analysis was used to assess the separable influences of activation and connector-hub status on task-state

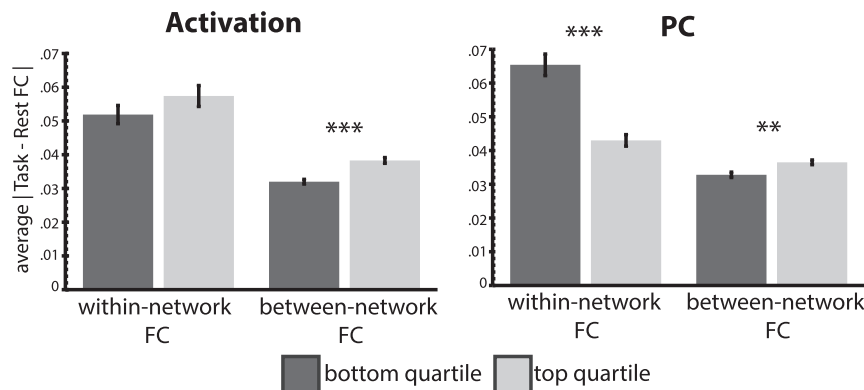


Figure 4. FC Modulations in Activated Regions and Connector Hubs

Active (left) and connector hub nodes (right) show significantly enhanced modulations in between-network FC, but not within network FC—instead, connector hubs show lower changes in within-system FC than non-connectors nodes. Similar effects were seen for individual tasks (Figure S5). *** $p < 0.001$, ** $p < 0.01$, error bars represent SE across ROIs.

changes in FC, with terms for activation, participation coefficient, and the interaction of both properties (Table S3; activation and PC were not themselves correlated, Spearman’s $\rho = 0.08$, $p = 0.23$, Figure S3C). As before, activation had a significant positive relationship with task-based changes in FC across the brain ($p < 0.001$), in this case both within ($p < 0.01$) and between networks ($p < 0.001$). PC had a significant negative relationship with within-network FC changes ($p < 0.001$) and a positive relationship with between-network FC changes ($p < 0.001$). However, no significant interactions were seen (all $p = n.s.$). These findings indicate that PC and activation provide separable, additive, contributions to modulations of FC during tasks.

Node Classes Show Distinct FC Attributes

In order to characterize how activation and PC relate to task-control and processing, we identified four classes of nodes from the extremes of each distribution: (1) silent simple nodes (in the bottom 25% of both activation and PC), (2) activated connector nodes (top 25% of activation and PC), (3) activated simple nodes (top 25% activation and bottom 25% PC), and (4) silent connector nodes (top 25% PC and bottom 25% activation). Notably, activation and PC were continuously distributed, but the distributions had heavy tails, suggesting that extreme PC and activation values may exhibit specialized characteristics.

The four classes were found in distinct locations (Figure 5). Activated connectors ($N = 20$) were primarily in top-down control systems, including the frontoparietal (FP), dorsal attention (DAN), cinguloopercular (CO), and salience systems. Silent connectors ($N = 9$) were also found in control systems (CO, salience, FP, as well as auditory regions abutting the CO network), but in secondary locations, e.g., posterior insula portions of the CO network and rostral portions of the FP. The activated simple class ($N = 16$) was associated with processing systems (visual, SM, DMN) that were relevant for the present tasks. Finally, the silent simple class ($N = 14$) was also associated with processing systems (SM, lat-SM, and the DMN). The association of the four classes with different networks suggests that they may carry out different roles in task control and processing.

Furthermore, we examined how classes varied across attributes—the FC change magnitude, topography, and variability across tasks—that would be expected to differ between regions involved in task control and processing. Specifically, regions that

enact task control are predicted to show high between-system FC, especially with processing systems relevant for a given task and flexibility in their patterns across

tasks with different goals. Regions involved in basic task processing, instead, are predicted to show high FC-modulations with both control regions and regions within their own system. Additionally, they should show stereotyped FC patterns regardless of task context. We find that each class was associated with distinct FC-attributes, arguing that classes relate to distinct processes for modifying brain networks (summary in Figure 6D).

Magnitudes of FC Modulations

The four classes differed in the absolute magnitude of FC changes within ($F(3,55) = 9.67$, $p < 0.001$) and between ($F(3,55) = 10.55$, $p < 0.001$) each network (Figure 6A; tested with a between-group ANOVA of the effect of class on FC change magnitude). Compared with the silent simple class, activated simple nodes had enhanced within- and between-network FC during tasks. Activated connectors, instead, had relatively smaller changes in within-network FC, but the highest levels of between-network FC changes. Finally, silent connector showed the most stable within-network FC and only modest changes in between-network FC.

Topography of FC Modulations

The four classes differed in the topography of their FC changes (measured as the average FC between regions in each class and target systems after removing values < 20 mm from a seed; Figure 6C). During the task, the activated connector class had greater FC with control systems and processing regions relevant to the task (i.e., visual and SM regions used for stimulus input and motor output in the tasks), but decreased FC with the DMN. By contrast, the activated simple class exhibited two major patterns: visual regions had decreased task FC with other visual regions and increased FC with control systems, while the DMN regions exhibited increased FC within their own network, but decreased connectivity with control regions. Silent connectors, on average, were not modulated across the major groups of networks (see Figure 7 for details on a subset). Finally, the silent simple class had decreased FC with processing regions but few increases (see Figure S7 for maps and quantification of the dominant patterns exhibited by regions within each class).

Flexibility of FC Modulations

Finally, we asked if classes were equally “flexible” in adjusting their pattern of connections across task states, as would be predicted for regions that modify distributed brain processing to achieve different goals. “Flexibility” was quantified by computing the correlation of whole-brain FC differences (task-rest) between

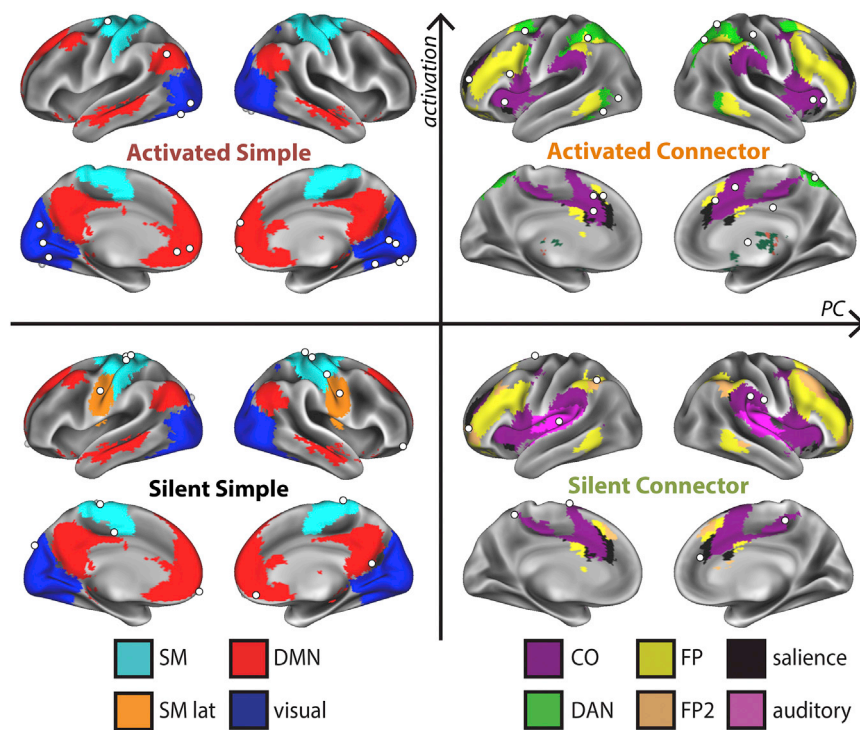


Figure 5. Regions Stratified into Classes by Activated and Connector Hub Characteristics

Regions were stratified into four classes: silent simple (bottom 25% of both activation and PC), activated simple (top 25% activation, bottom 25% PC), silent connector (bottom 25% activation, top 25% PC), and activated connector (top 25% activation and PC) nodes. Node locations are shown as white spheres overlaid on their systems (colors). Classes were associated with distinct systems.

we tested whether network changes were related to (1) the activation of a region, or (2) a region's topological hub properties. We found evidence that both properties provide separate, additive contributions to changes in FC in tasks varying from semantic judgments and mental rotation to visual coherence assessments. Activated regions showed higher connectivity than non-activated regions, especially between networks. Connector-hubs also had large modulations of between-network FC, but relatively invariant within-network FC. Regions stratified

the three tasks; lower correlations should indicate relatively more flexibility in FC modulation across tasks. Classes differed significantly in their flexibility (between-group ANOVA: $F(3,55) = 9.35$, $p < 0.001$). The activated simple class had relatively low flexibility in the pattern of changes across tasks, similar to that seen with silent simple nodes. By contrast, activated and silent connectors both showed relatively high flexibility across tasks (Figure 6B; all two-sample t tests between simple and connector classes, $p[\text{FDR}] < 0.01$, corrected for six comparisons between classes).

Comparing across Classes within a Single Network

Many of the divergent patterns of FC modulation were associated with nodes from distinct networks. However, we observed that, in some cases, regions from the same network, but different classes, also showed systematically different FC changes. For example, we compared activated ($N = 7$) and silent ($N = 4$) connector nodes in the CO network (Figure 7A; this comparison yielded the highest N in two separate classes). The two classes differed in their pattern of network modulations, clustering separately (Figure 7B). Moreover, direct comparison showed that activated connectors had relatively higher FC with control systems (FP, DAN) and the visual processing system, but relatively lower FC with the DMN (two-sample t test; Figure 7C). This provides evidence that node class, determined by activation and connector-hub status, relates to differences in task-FC even in cases where nodes are from the same network.

DISCUSSION

Despite a largely preserved network organization, we found reliable small-scale differences between task and rest FC. Critically,

into different classes based on their activation and connector-hub status were localized to distinct networks and showed significantly different patterns of FC changes, suggesting that they are associated with distinct processes for modulating FC during tasks.

An Intrinsic Network Structure Dominates Rest and Task States, but Individual Connections Show Reliable Differences

FC networks and network properties were very similar between task and rest states, consistent with past reports (Betti et al., 2013; Cole et al., 2014; Krienen et al., 2014). These findings indicate that functional networks are dominated by stable, intrinsic correlation patterns that do not substantially change under different states of consciousness (Greicius et al., 2008; Larson-Prior et al., 2009) or task engagement (Cole et al., 2014). This stable backbone may be driven by anatomical connectivity between regions as well as the statistical history of co-activations that regions exhibit across the lifespan (Dosenbach et al., 2007).

However, although quite similar, subtle but systematic differences were present between rest and task networks, as suggested by previous examinations of an expanse of tasks (Betti et al., 2013; Cole et al., 2014), including internally motivated tasks that share many similarities with rest (Krienen et al., 2014; Shirer et al., 2012). We found FC differences both within and between systems, including in processing (e.g., visual), control (e.g., subsets of frontoparietal and cinguloopercular), and default mode systems.

Our tasks differed in detailed aspects of their FC, but prominent changes were consistent across all three tasks. These FC

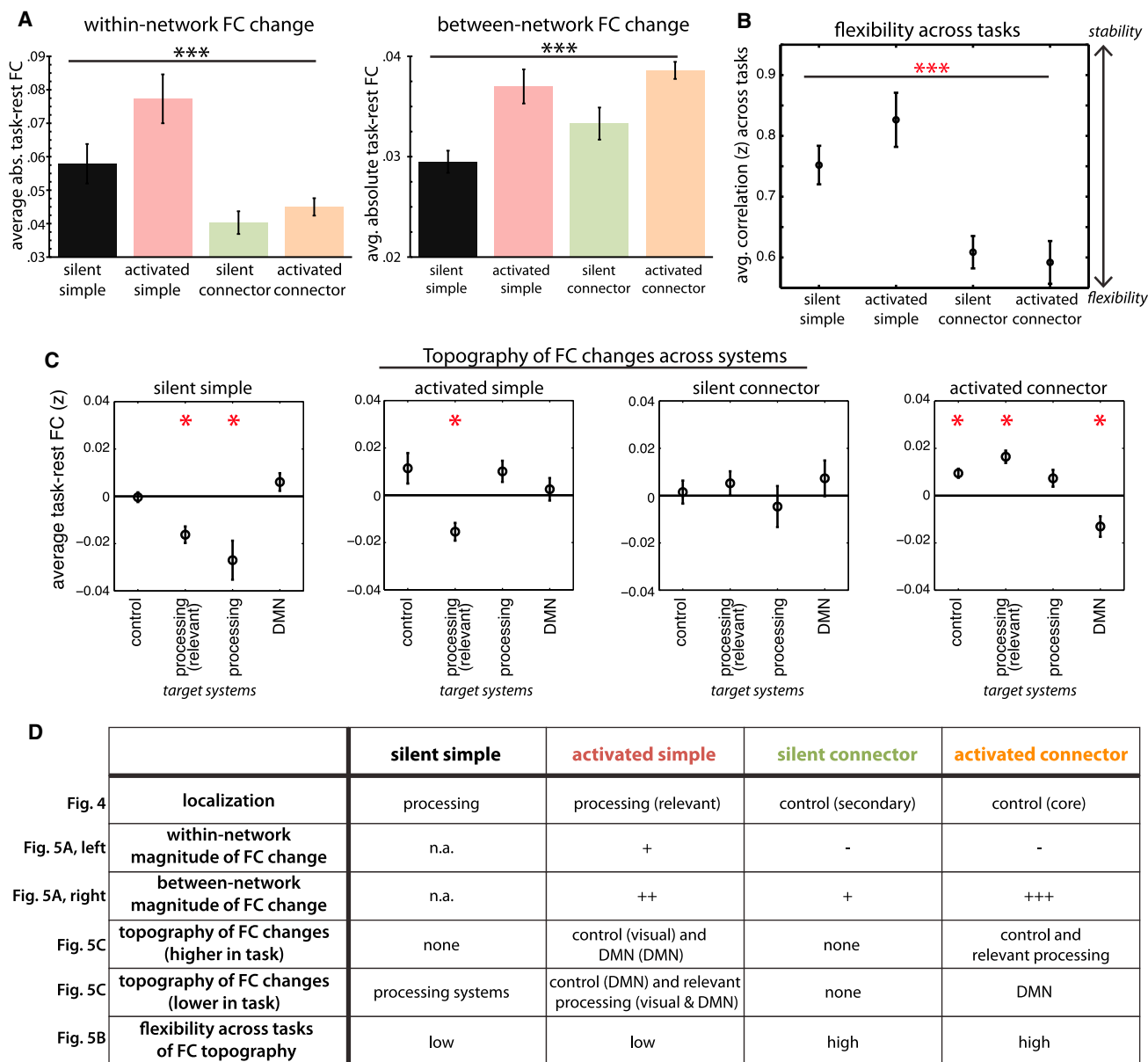


Figure 6. Classes Differ in the Magnitude, Topography, and Flexibility of Their FC Patterns

Node classes had different FC-related attributes.

(A) Classes differed in the absolute magnitude of within and between network FC changes (measured via one-way ANOVA, $***p < 0.001$).

(B) Classes differed in the flexibility of their topography across tasks, measured as the average correlation among FC difference maps for each class.

(C) Classes differed in the topography of FC differences across networks, quantified via the FC task-rest difference for a class of regions (source) to each brain network (target; * $p[\text{FDR}] < 0.05$; control, CO, salience, FP, DAN, VAN; relevant processing, visual, SM; processing, lat-SM, auditory).

(D) These attributes, and the figures associated with each, are summarized in (D); absolute magnitudes of FC changes are shown with increasing \pm signs relative to silent simple nodes to denote increasingly large differences). Error bars represent SE across ROIs.

changes were associated with different classes of nodes, defined by nodes' activation and connector-hub properties, and are discussed in more detail below. Although our tasks varied substantially in their nature (including verbal and non-verbal stimuli, varying levels of perceptual demands, varying levels of difficulty, and varying involvement of control systems) (Dubis et al., 2016), they did not fully sample the space of tasks that

humans can complete. All of the tasks had visual inputs, had motor responses, and used a mixed-block/event-related design. Future tests will be needed to establish whether any elements of these findings are dependent on the commonalities present across these tasks and, additionally, what properties may drive network differences between tasks (Cole et al., 2014; Krienen et al., 2014).

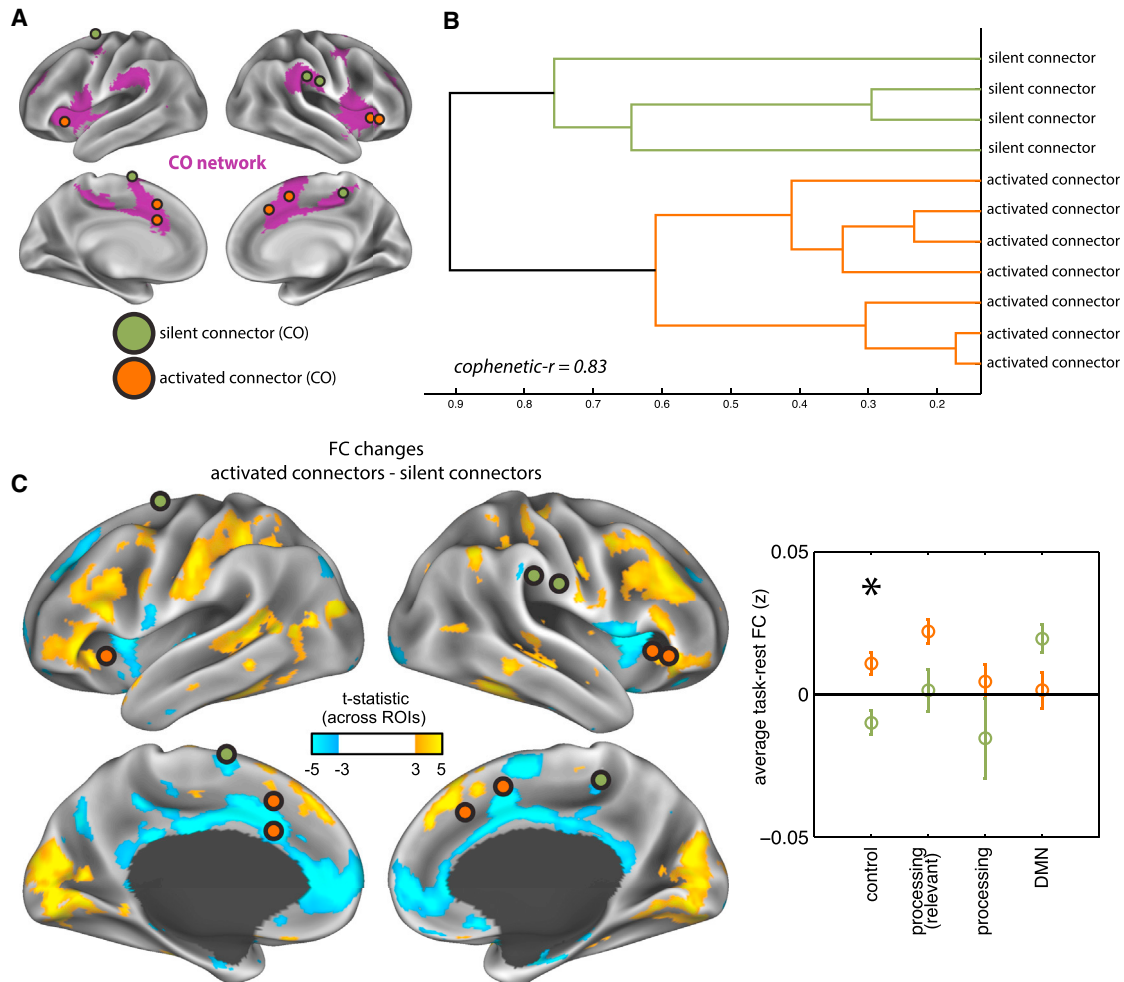


Figure 7. Nodes within the CO Network Show Distinct FC Patterns Based on Their Class

(A) Regions associated with different classes showed distinct patterns of FC modulations, even when they were part of the same network. For example, we contrast the pattern of FC modulations (task-rest) exhibited by activated connectors (N = 7, orange) and silent connectors (N = 4, green) that are part of the CO network (purple; A).

(B) Classes clustered separately from one another based on their FC difference maps.

(C) Activated connector CO regions showed increased coupling with FP, DAN, and visual regions relative to silent connector CO regions (quantified in left panel for different types of networks; *p[FDR] < 0.05; see Figure 6 for network groupings). Error bars represent SE across ROIs.

Modulations of Brain Networks Are Related to Both the Functional and Topological Properties of Each Region

Having found reliable connectivity changes between task and rest, we investigated whether altered FC is more associated with the functional (activation) characteristics of regions (Hypothesis 1) or the topological properties (connector-hub status) of regions within large-scale networks (Hypothesis 2). We found evidence that both the activation of a region and the region's putative hub role was related to changes in FC during a task.

Activation

Intuitively, one might assume that changes in FC will perfectly reflect activation during a task. Indeed, many past studies have focused on studying FC among small sets of activated (or de-activated) areas. For example, in visual attention tasks, interactions are altered among visual association regions and fronto-

parietal cortex (Gazzaley et al., 2007), the default mode (Chadick and Gazzaley, 2011), and other visual areas (Al-Aidroos et al., 2012), that all show either enhanced or suppressed activity during the task. Analogously, other studies have examined FC among regions activated in long-term memory (King et al., 2015), executive function (Elton and Gao, 2014), and working memory tasks (Cohen et al., 2014; Fransson, 2006; Hampson et al., 2006; Newton et al., 2011).

We examined the assumption adopted in these studies, that task-active regions will show significant changes in FC, by systematically measuring the relationship between activation in these three tasks and FC throughout the brain. Activated regions had greater changes in FC during tasks than non-activated regions, especially between networks. This effect was consistent across our tasks, various analysis approaches,

and parcellation schemes, extending the generalizability of our results beyond previous findings limited to a small number of connections in a single task context (i.e., tasks spanning semantic judgments, mental rotations, and visual coherence). These findings indicate that system-level network changes accompany, and may facilitate, local processing during tasks (see also Bassett et al., 2012; Siebenhüner et al., 2013; Zalesky et al., 2012).

In general, it is notable that activation and FC were not perfectly correlated with one another. This finding emphasizes that while activation and correlation measures may be related, they appear to index separable aspects of brain function—one encapsulating first order statistics of local neural responses and the other capturing second order statistics reflecting how variations in neural activity may be related across distributed regions.

Finally, it remains unclear whether the task-based alterations seen in this manuscript reflect sustained state-based changes in network correlations or trial-to-trial variability of evoked responses that is correlated across regions (Rissman et al., 2004) or, indeed, if these two hypotheses are dissociable, as fluctuations in activity between intrinsically correlated regions help explain trial-to-trial evoked response variability (Fox et al., 2007). Future research will be needed to differentiate between these two possibilities and their implications for functional networks.

Connector Hubs

In addition to activation, we demonstrate that the hubs are also central to understanding network modulations in tasks. Connector hubs are defined by having strong connections to multiple brain systems; here we show they also have strong changes in between-system FC during tasks. This ability to modify interactions between distributed systems may be central to completing complex tasks such as the ones examined here (Mesulam, 1990). Our findings link to prior evidence that has also suggested that connector hubs are important for cognition. Brain lesions to connector hubs lead to pervasive behavioral deficits (Warren et al., 2014) and connector hubs show a diverse activation profile across different cognitive processes (Bertolero et al., 2015). Further, Cole et al. (2013) found that the FP network, characterized as having many connector-hubs, showed variable between-system FC across tasks. We demonstrate that connector hubs throughout the brain, in many control systems, show high FC modulation across these three tasks. Moreover, these hub effects are separate from the effects of task activation and exhibit distinct FC-related attributes, suggesting that hub status and task activation index separate factors for modifying brain networks.

Perhaps surprisingly, connector hubs had significantly less absolute change in their within-network FC. While robust, this result is less clearly predicted from previous literature. Perhaps high within-network invariance allows connector hubs to maintain a more veridical tie to the functional processing of their own network, while mediating malleable interactions with other networks. Regardless of their cause, these findings indicate that connector hubs are able to more finely tune their FC, compared with activated regions, as some connections are selectively modified while others are kept constant.

Dissociable Factors for Task-Based Network Modulation

Activation and PC provided separable, additive contributions to network changes during the three tasks examined here, suggesting they relate to dissociable factors for network modulation. To characterize these complementary processes, we examined classes of regions, stratified based on their activation and connector hub status. The classes exhibited a number of distinct attributes, including in their locations, the topography of their network changes, and the flexibility of this topography across task contexts. Although we cannot identify the specific neural processes employed based on these data, the distinct characteristics exhibited by activated and connector hub nodes argue for the presence of at least two dissociable mechanisms for linking brain regions together during complex tasks such as these. We propose that the classes are differentially linked to enacting task control and to conducting task processing.

Activated Connectors

Activated connectors, regions that were both activated and connector hubs, exhibited characteristics consistent with a role in enacting control. During tasks, these regions had the largest absolute magnitude of network changes between systems and the smallest changes within a system, suggesting a substantial but finely tuned manipulation of network connectivity. Activated connectors were found primarily in “control” systems, which have been implicated in a variety of attention- or top-down-related functions, including goal-directed attention (DAN) (Corbetta and Shulman, 2002), detection of salient events (salience) (Seeley et al., 2007), and task control at multiple time-scales (CO, FP) (Dosenbach et al., 2007, 2008).

Activated connectors had pronounced increases in FC with processing regions that were relevant for our tasks (visual, SM systems), a topography consistent with “control” systems that exert top-down signaling adjustments on relevant processing systems in the service of task goals (Petersen and Posner, 2012). A separate literature has also found lower FC between control systems (especially the DAN) and the DMN during tasks, as we found here (Bluhm et al., 2011; Kelly et al., 2008; Newton et al., 2011; Wang et al., 2012). Fewer studies have examined the interactions across different control systems during tasks (but see Cohen et al., 2014)—we show that subsets of these systems become more integrated, despite their independent pattern at rest (Dosenbach et al., 2007; Nomura et al., 2010).

Finally, activated connectors had variable patterns of FC changes across tasks, consistent with the expectation that control regions should show flexibility in network modulations in different task contexts, given differences in their control and processing demands (see Dubis et al., 2016 on these tasks).

The attributes of activated connectors were distinct from those of other classes, underscoring the importance of both activation and connector-hub properties for understanding how brain regions interact during tasks.

Activated Simple Class

This class contained regions in processing systems, including the visual system and a hand-SM region. Unlike activated connectors, this class showed high levels of both within- and between-system modifications and their pattern of FC changes had low flexibility across tasks. These attributes are consistent

with basic task-processing regions that alter interactions both with control regions in other networks and processing regions in their own network, but in a stereotyped way regardless of the specific task context.

In this class, the topography of network changes varied substantially by system. Visual regions had decreased visual correlations, but increased correlations to other (especially control) systems, as in previous reports (Betti et al., 2013; Spadone et al., 2015). DMN regions, instead, had decreased correlations with other, especially control, systems (Bluhm et al., 2011; Kelly et al., 2008; Newton et al., 2011; Wang et al., 2012) and increased within system correlations during tasks. The literature is mixed on how tasks affect FC within the DMN (Betti et al., 2013; Fransson, 2006; Hampson et al., 2006; Newton et al., 2011), perhaps due to differences in task design or the portions of the DMN examined. We speculate that both the visual and DMN effects reflect a relatively more isolated, modular, state for the system—coherence within the system core and segregation from other systems—when not called upon (i.e., during the task for DMN, during rest for the visual system). Indeed, the placement of DMN regions in the activated simple class and their shared characteristics with visual regions suggests that they are closely related to processing, rather than control, systems.

Silent Connectors

Silent connectors shared some attributes with activated connectors (invariant within-network FC, high flexibility in FC patterns across tasks, and localization to control systems). However, relative to activated connectors, silent connectors had weaker magnitudes of between-network FC and a distinct FC topography (e.g., a lack of FC to visual systems and, in CO silent connectors, decreased FC with control systems) (Figure 7). Moreover, silent connectors were found in less well-studied regions of control systems (i.e., the mid-cingulate and posterior insula portions of the CO, rostral frontal portions of the FP). These regions may be associated with control of different types of tasks than we and others have examined; alternatively they may have a distinct role in task processing than the well-studied “core” sections (Dosenbach et al., 2006) associated with activated connectors.

Silent Simple Class

Silent simple regions were neither task-activated nor connector hubs; therefore, neither hypothesis would expect strong changes in these regions—indeed, we found weak changes in these regions, primarily associated with decreased FC in processing systems.

Conclusions

Although dominated by a stable intrinsic backbone, large-scale networks differ systematically between three distinct tasks and rest. We tested two hypotheses for which locations would show large changes in functional connectivity: regions activated in a task or regions that serve as connector hubs for transferring information across systems. We found evidence that the properties provide separate contributions to network changes. Furthermore, classes of regions defined by their activation and connector-hub status were located in different networks and exhibited different magnitudes, topography, and variability of FC modulations. In particular, “activated connector” regions ex-

hibited attributes consistent with a role in enacting task control. These findings argue for the presence of at least two dissociable factors related to functional specialization and network hubs that contribute to changes in coordination among distributed brain regions during different task contexts.

EXPERIMENTAL PROCEDURES

Participants

Task and resting-state data were collected from 29 healthy young participants (15 female, average age 25 years, range 21–30 years). Task data was previously published (Dubis et al., 2016), and a subset of the resting-state data was included in a larger cohort reported in Power et al. (2011). After censoring high-motion time points (Power et al., 2014), one participant was dropped for the task (concatenated data from all task conditions) versus rest comparisons, and four participants were dropped from examinations of single task data due to insufficient remaining time points (<120). Written informed consent was obtained from all participants, who were compensated monetarily for their participation. Procedures were approved by the Institutional Review Board at Washington University in St. Louis.

Tasks

Participants completed three tasks in a mixed block/event-related design: a semantic task (noun/verb judgment on a word), a mental rotation task (same/mirror image judgment on two 3-D objects), and a coherence judgment task (judgment of whether a set of dots arranged were concentrically). The tasks differed substantially from one another, including either verbal or non-verbal stimuli or required different perceptual and control demands (Dubis et al., 2016). Furthermore, a substantial amount of data was present for each task (~23 min per task, >1 hr total), providing reliable measures of whole-brain task FC (Laumann et al., 2015). See the [Supplemental Experimental Procedures](#) for details on behavioral paradigms and stimuli.

Resting State

During resting-state scans, participants lay quietly in the scanner while passively viewing a fixation cross. Between 10 and 140 min (average = 50 min) of total resting state data were collected from each participant, 10–20 min of which were from the same session as the task data. When available (N = 23/29 participants), resting state data was supplemented from other experimental sessions.

Image Acquisition Parameters

Data was acquired on a Siemens 3T Trio at Washington University in St. Louis, using a 12-channel head coil. A high-resolution structural image was acquired from each participant using a sagittal magnetization-prepared rapid gradient echo (MP-RAGE) sequence (slice time echo = 3.08 ms, TR = 2.4 s, inversion time = 1 s, flip angle = 8°, 176 slices, 1 × 1 × 1 mm voxels). Functional images were acquired using an asymmetric spin-echo echo-planar pulse sequence (TR = 2.5 s, TE = 27 ms, flip angle = 90°, 4 × 4 mm in-plane resolution). Whole brain coverage was achieved using 32 contiguous interleaved 4-mm slices aligned parallel to the anterior-posterior commissure. These parameters were identical for all task and rest sessions.

Data was initially processed using standard techniques to reduce artifacts (Miezin et al., 2000) (including slice-time correction, alignment, intensity normalization, and transformation to atlas space; see the [Supplemental Experimental Procedures](#) for details).

FC Processing

Both resting and task data were analyzed using a FC approach. First, task-evoked activity was removed from task time series by applying the GLM model described below and extracting the residuals from the model. Importantly, this approach reduces spurious correlations induced by task activations and highlights underlying changes in connectivity that are present throughout a period of task performance (i.e., “background” connectivity) (Al-Aidroos et al., 2012). Note that the overall pattern of FC changes were quite similar whether task FC was calculated based on residuals or raw data (Figure S4A), although as

expected, estimates of their relationship to activation were inflated (Figure S4B). Tasks were analyzed both individually and as a unit (concatenated across tasks).

FC processing was applied to both task and resting-state time series. Processing followed Power et al. (2014), including regression of nuisance signals from white matter, cerebral spinal fluid, global signal, and motion parameters, spatial and temporal filtering, and censoring of high motion frames (>0.2 mm; the Supplemental Experimental Procedures). Following this, Pearson correlations were calculated between average time series from regions of interest. In task FC analyses, only frames from relevant task periods were included in the correlations. Notably, functional connectivity measures are related to anatomical connectivity (Honey et al., 2009), but do not necessarily reflect direct anatomical connections between brain regions.

Regions and Networks

FC analyses were computed among 264 regions of interest (10-mm diameter spheres) across the brain spanning cortical and subcortical locations (Power et al., 2011) (Figure 2A). These regions are associated with 13 networks based on previous work (Power et al., 2011): somatomotor (SM), lateral somatomotor (lat-SM), cinguloopercular (CO), auditory, default mode (DMN), memory, visual, frontoparietal (FP), salience, sub-cortex, ventral attention (VAN), dorsal attention (DAN), and cerebellum, as well as a group of undefined regions. In this and previous work (Power et al., 2011), regions were sorted into networks using the Infomap random walk clustering algorithm (Rosvall and Bergstrom, 2008) based on weighted correlation matrices across a range of sparsity thresholds (2%–10% for 264 regions of interest [ROIs], 0.5%–5% for voxelwise networks). To algorithmically define consensus networks from this dataset for comparison to Power et al. (2013), we placed regions in networks using data from the lowest threshold, but excluding small networks (<4 nodes or 400 voxels). Higher thresholds were examined in turn to assign networks to voxels that remained unaffiliated.

Analyses were additionally completed on 333 parcels produced through novel surface-based FC boundary mapping methods (Gordon et al., 2016) and on modified voxelwise graphs (Power et al., 2011) to show consistency between approaches. All ROI and voxelwise analyses were conducted on volume-space data but are projected onto the surface for visualization purposes.

General Linear Model of Task Activation

We modeled task activations using a general linear model (GLM) approach to determine how task-FC was altered in activated regions. Modeling was conducted on individual voxels using in-house imaging software. The GLM model included linear and constant terms for each run to remove baseline and drift effects. In addition, the following task events were modeled: start cues, end cues, trials coded by accuracy and type (i.e., noun and verb for the semantic task, three different orientation bins for the mental rotation task, and four different coherence conditions for the coherence task), and sustained task responses. Sustained responses were modeled as a block effect. For cue and trial conditions, ten individual time points (25-s) were modeled with delta functions to describe the full temporal extent of the hemodynamic response. This approach makes no assumptions about the shape of the hemodynamic response (Ollinger et al., 2001), allowing us to fully model (and subsequently remove) evoked activations even when response shapes may differ. Activations from modeling were expressed as a percent signal change, dividing the magnitude of activation by the baseline term for each run. Average activations for each region were computed as a weighted average of all correct task conditions (cue, trial, and sustained); all conditions were included as FC was examined over the entire task).

Comparing Correlation Matrices

Correlation values were Fisher z transformed. Similarity between FC matrices was evaluated by correlating FC values and by computing Mantel's statistic. Differences between FC matrices were quantified using two approaches that provided a mixture of generalized and edge-specific measurements. First, a paired two-sided t test was conducted for each unique entry in the FC matrix. The distribution of t test p values was compared to a null-distribution determined by permuting task and rest states. Second, individual t tests were subjected to false discovery rate (FDR) correction for

multiple comparisons to identify connections that significantly differed between conditions.

FC Change per Region

The average absolute change in FC for a given region was computed by taking the mean of the absolute correlation differences between task and rest for that region to every other region. We also examined within- and between-network changes in FC separately by computing the mean of a region's absolute FC difference to other regions within its own network (within-network) or to regions in other networks (between network). The majority of analyses were computed using the 264 ROIs and networks introduced above. We also made similar computations for voxelwise graphs, where group-average connectivity differences were computed for each voxel to every other voxel (all connections), all other voxels assigned to the same network (within-network), or voxels assigned to other networks (between-network). Voxelwise summaries were used for qualitative representation of the anatomical locations of effects, not quantification.

Relationship between FC and Activation/PC

We used a quartile analysis to compare activated/connector hub regions (those in the top 25% of the activation/PC distribution; see the Supplemental Experimental Procedures for PC definition) to low activation/non-connectors (those in the bottom 25% of the activation/PC distribution). Regions with low signal and uncertain network assignment ("unassigned") (Power et al., 2011) were excluded from these and following analyses. For each sample of ROIs, we compared FC changes using non-parametric permutation tests where ROI labels (top, bottom quartile) were permuted. In a second approach, we correlated FC changes for each region with continuous measures of activation/PC, using Spearman's correlations. Finally, we used a linear regression analysis, with Z scored regressors for activation and PC as well as their interaction, to jointly examine the two properties. For simplicity, only linear relationships were tested in correlations/regression (scatterplots are available in Figure S6); however, quartile analyses do not depend on linear assumptions. For these and following analyses when more than two comparisons were made, p values were FDR-corrected for multiple comparisons (i.e., across tasks, across classes).

We also examined the attributes of classes of regions with combinations of different properties: (1) "activated connectors" (top 25% of both PC and activation), (2) "silent connectors" regions (top 25% of PC, bottom 25% activation), (3) "activated simple nodes" (top 25% activation, bottom 25% PC), and (4) "silent simple nodes" (bottom 25% of both activation and PC). We (1) determined the network identities of nodes in each class, (2) measured the absolute magnitude of within and between FC changes, (3) measured the topography, and (4) flexibility of FC changes. Results were compared across classes using one-way between-factor ANOVAs and post hoc using two-sample t tests FDR corrected for multiple comparisons. See the Supplemental Experimental Procedures for details on these analyses and on analyses comparing activated and silent connectors in the CO network.

SUPPLEMENTAL INFORMATION

Supplemental Information includes Supplemental Experimental Procedures, eight figures, and three tables and can be found with this article online at <http://dx.doi.org/10.1016/j.celrep.2016.10.002>.

AUTHOR CONTRIBUTIONS

C.G. and S.E.P. conceived of the study and secured funding. C.G. performed analyses. T.O.L., E.M.G., and B.A. provided software and feedback. C.G., T.O.L., E.M.G., B.A., and S.E.P. wrote the manuscript.

ACKNOWLEDGMENTS

We thank Joe Dubis, Rebecca Coalson, Fran Miezin, and Mark McAvooy for technical assistance. This research was supported by a McDonnell Foundation Collaborative Activity Award (S.E.P.), NIH R01NS32979 (S.E.P.), NIH

R01NS06424 (S.E.P.), NIH T32NS0007205-33, and F32NS092290 (C.G.), and was supported in part by the Neuroimaging Informatics and Analysis Center (1P30NS098577).

Received: May 5, 2016

Revised: September 1, 2016

Accepted: September 24, 2016

Published: October 25, 2016

REFERENCES

- Al-Aidroos, N., Said, C.P., and Turk-Browne, N.B. (2012). Top-down attention switches coupling between low-level and high-level areas of human visual cortex. *Proc. Natl. Acad. Sci. USA* *109*, 14675–14680.
- Alnæs, D., Kaufmann, T., Richard, G., Duff, E.P., Sneve, M.H., Endestad, T., Nordvik, J.E., Andreassen, O.A., Smith, S.M., and Westlye, L.T. (2015). Attentional load modulates large-scale functional brain connectivity beyond the core attention networks. *Neuroimage* *109*, 260–272.
- Bassett, D.S., Nelson, B.G., Mueller, B.A., Camchong, J., and Lim, K.O. (2012). Altered resting state complexity in schizophrenia. *Neuroimage* *59*, 2196–2207.
- Bertolero, M.A., Yeo, B.T., and D'Esposito, M. (2015). The modular and integrative functional architecture of the human brain. *Proc. Natl. Acad. Sci. USA* *112*, E6798–E6807.
- Betti, V., Della Penna, S., de Pasquale, F., Mantini, D., Marzetti, L., Romani, G.L., and Corbetta, M. (2013). Natural scenes viewing alters the dynamics of functional connectivity in the human brain. *Neuron* *79*, 782–797.
- Biswal, B., Yetkin, F.Z., Haughton, V.M., and Hyde, J.S. (1995). Functional connectivity in the motor cortex of resting human brain using echo-planar MRI. *Magn. Reson. Med.* *34*, 537–541.
- Bluhm, R.L., Clark, C.R., McFarlane, A.C., Moores, K.A., Shaw, M.E., and Lanius, R.A. (2011). Default network connectivity during a working memory task. *Hum. Brain Mapp.* *32*, 1029–1035.
- Chadick, J.Z., and Gazzaley, A. (2011). Differential coupling of visual cortex with default or frontal-parietal network based on goals. *Nat. Neurosci.* *14*, 830–832.
- Cohen, J.R., Gallen, C.L., Jacobs, E.G., Lee, T.G., and D'Esposito, M. (2014). Quantifying the reconfiguration of intrinsic networks during working memory. *PLoS ONE* *9*, e106636.
- Cole, M.W., Reynolds, J.R., Power, J.D., Repovs, G., Anticevic, A., and Braver, T.S. (2013). Multi-task connectivity reveals flexible hubs for adaptive task control. *Nat. Neurosci.* *16*, 1348–1355.
- Cole, M.W., Bassett, D.S., Power, J.D., Braver, T.S., and Petersen, S.E. (2014). Intrinsic and task-evoked network architectures of the human brain. *Neuron* *83*, 238–251.
- Corbetta, M., and Shulman, G.L. (2002). Control of goal-directed and stimulus-driven attention in the brain. *Nat. Rev. Neurosci.* *3*, 201–215.
- Dosenbach, N.U., Visscher, K.M., Palmer, E.D., Miezin, F.M., Wenger, K.K., Kang, H.C., Burgund, E.D., Grimes, A.L., Schlaggar, B.L., and Petersen, S.E. (2006). A core system for the implementation of task sets. *Neuron* *50*, 799–812.
- Dosenbach, N.U., Fair, D.A., Miezin, F.M., Cohen, A.L., Wenger, K.K., Dosenbach, R.A., Fox, M.D., Snyder, A.Z., Vincent, J.L., Raichle, M.E., et al. (2007). Distinct brain networks for adaptive and stable task control in humans. *Proc. Natl. Acad. Sci. USA* *104*, 11073–11078.
- Dosenbach, N.U., Fair, D.A., Cohen, A.L., Schlaggar, B.L., and Petersen, S.E. (2008). A dual-networks architecture of top-down control. *Trends Cogn. Sci.* *12*, 99–105.
- Dubis, J.W., Siegel, J.S., Neta, M., Visscher, K.M., and Petersen, S.E. (2016). Tasks driven by perceptual information do not recruit sustained BOLD activity in cingulo-opercular regions. *Cereb. Cortex* *26*, 192–201.
- Dwyer, D.B., Harrison, B.J., Yücel, M., Whittle, S., Zalesky, A., Pantelis, C., Allen, N.B., and Fornito, A. (2014). Large-scale brain network dynamics supporting adolescent cognitive control. *J. Neurosci.* *34*, 14096–14107.
- Elton, A., and Gao, W. (2014). Divergent task-dependent functional connectivity of executive control and salience networks. *Cortex* *51*, 56–66.
- Fox, M.D., Snyder, A.Z., Vincent, J.L., and Raichle, M.E. (2007). Intrinsic fluctuations within cortical systems account for intertrial variability in human behavior. *Neuron* *56*, 171–184.
- Fransson, P. (2006). How default is the default mode of brain function? Further evidence from intrinsic BOLD signal fluctuations. *Neuropsychologia* *44*, 2836–2845.
- Gazzaley, A., Rissman, J., Cooney, J., Rutman, A., Seibert, T., Clapp, W., and D'Esposito, M. (2007). Functional interactions between prefrontal and visual association cortex contribute to top-down modulation of visual processing. *Cereb. Cortex* *17* (Suppl 1), i125–i135.
- Gonzalez-Castillo, J., Hoy, C.W., Handwerker, D.A., Robinson, M.E., Buchanan, L.C., Saad, Z.S., and Bandettini, P.A. (2015). Tracking ongoing cognition in individuals using brief, whole-brain functional connectivity patterns. *Proc. Natl. Acad. Sci. USA* *112*, 8762–8767.
- Gordon, E.M., Breeden, A.L., Bean, S.E., and Vaidya, C.J. (2014). Working memory-related changes in functional connectivity persist beyond task disengagement. *Hum. Brain Mapp.* *35*, 1004–1017.
- Gordon, E.M., Laumann, T.O., Adeyemo, B., Huckins, J.F., Kelley, W.M., and Petersen, S.E. (2016). Generation and evaluation of a cortical area parcellation from resting-state correlations. *Cereb. Cortex* *26*, 288–303.
- Gratton, C., Nomura, E.M., Pérez, F., and D'Esposito, M. (2012). Focal brain lesions to critical locations cause widespread disruption of the modular organization of the brain. *J. Cogn. Neurosci.* *24*, 1275–1285.
- Greicius, M.D., Kiviniemi, V., Tervonen, O., Vainionpää, V., Alahuhta, S., Reiss, A.L., and Menon, V. (2008). Persistent default-mode network connectivity during light sedation. *Hum. Brain Mapp.* *29*, 839–847.
- Guimera, R., and Amaral, L.A. (2005). Cartography of complex networks: modules and universal roles. *J. Stat. Mech.* *2005*, P02001-1–P02001-13.
- Hampson, M., Tokoglu, F., Sun, Z., Schafer, R.J., Skudlarski, P., Gore, J.C., and Constable, R.T. (2006). Connectivity-behavior analysis reveals that functional connectivity between left BA39 and Broca's area varies with reading ability. *Neuroimage* *31*, 513–519.
- Hampson, M., Driesen, N., Roth, J.K., Gore, J.C., and Constable, R.T. (2010). Functional connectivity between task-positive and task-negative brain areas and its relation to working memory performance. *Magn. Reson. Imaging* *28*, 1051–1057.
- Honey, C.J., Sporns, O., Cammoun, L., Gigandet, X., Thiran, J.P., Meuli, R., and Hagmann, P. (2009). Predicting human resting-state functional connectivity from structural connectivity. *Proc Natl Acad Sci USA* *106*, 2035–2040.
- Kelly, A.M., Uddin, L.Q., Biswal, B.B., Castellanos, F.X., and Milham, M.P. (2008). Competition between functional brain networks mediates behavioral variability. *Neuroimage* *39*, 527–537.
- King, D.R., de Chastelaine, M., Elward, R.L., Wang, T.H., and Rugg, M.D. (2015). Recollection-related increases in functional connectivity predict individual differences in memory accuracy. *J. Neurosci.* *35*, 1763–1772.
- Krienen, F.M., Yeo, B.T., and Buckner, R.L. (2014). Reconfigurable task-dependent functional coupling modes cluster around a core functional architecture. *Philos. Trans. R. Soc. Lond. B Biol. Sci.* *369*. <http://dx.doi.org/10.1098/rstb.2013.0526>.
- Larson-Prior, L.J., Zempel, J.M., Nolan, T.S., Prior, F.W., Snyder, A.Z., and Raichle, M.E. (2009). Cortical network functional connectivity in the descent to sleep. *Proc. Natl. Acad. Sci. USA* *106*, 4489–4494.
- Laumann, T.O., Gordon, E.M., Adeyemo, B., Snyder, A.Z., Joo, S.J., Chen, M.Y., Gilmore, A.W., McDermott, K.B., Nelson, S.M., Dosenbach, N.U., et al. (2015). Functional system and areal organization of a highly sampled individual human brain. *Neuron* *87*, 657–670.
- Mesulam, M.M. (1990). Large-scale neurocognitive networks and distributed processing for attention, language, and memory. *Ann. Neurol.* *28*, 597–613.
- Miezin, F.M., Maccotta, L., Ollinger, J.M., Petersen, S.E., and Buckner, R.L. (2000). Characterizing the hemodynamic response: effects of presentation

- rate, sampling procedure, and the possibility of ordering brain activity based on relative timing. *Neuroimage* 11, 735–759.
- Newton, A.T., Morgan, V.L., Rogers, B.P., and Gore, J.C. (2011). Modulation of steady state functional connectivity in the default mode and working memory networks by cognitive load. *Hum. Brain Mapp.* 32, 1649–1659.
- Nomura, E.M., Gratton, C., Visser, R.M., Kayser, A., Perez, F., and D'Esposito, M. (2010). Double dissociation of two cognitive control networks in patients with focal brain lesions. *Proc. Natl. Acad. Sci. USA* 107, 12017–12022.
- Ollinger, J.M., Corbetta, M., and Shulman, G.L. (2001). Separating processes within a trial in event-related functional MRI. *Neuroimage* 13, 218–229.
- Petersen, S.E., and Posner, M.I. (2012). The attention system of the human brain: 20 years after. *Annu. Rev. Neurosci.* 35, 73–89.
- Power, J.D., Cohen, A.L., Nelson, S.M., Wig, G.S., Barnes, K.A., Church, J.A., Vogel, A.C., Laumann, T.O., Miezin, F.M., Schlaggar, B.L., and Petersen, S.E. (2011). Functional network organization of the human brain. *Neuron* 72, 665–678.
- Power, J.D., Schlaggar, B.L., Lessov-Schlaggar, C.N., and Petersen, S.E. (2013). Evidence for hubs in human functional brain networks. *Neuron* 79, 798–813.
- Power, J.D., Mitra, A., Laumann, T.O., Snyder, A.Z., Schlaggar, B.L., and Petersen, S.E. (2014). Methods to detect, characterize, and remove motion artifact in resting state fMRI. *Neuroimage* 84, 320–341.
- Rissman, J., Gazzaley, A., and D'Esposito, M. (2004). Measuring functional connectivity during distinct stages of a cognitive task. *Neuroimage* 23, 752–763.
- Rosvall, M., and Bergstrom, C.T. (2008). Maps of random walks on complex networks reveal community structure. *Proc. Natl. Acad. Sci. USA* 105, 1118–1123.
- Seeley, W.W., Menon, V., Schatzberg, A.F., Keller, J., Glover, G.H., Kenna, H., Reiss, A.L., and Greicius, M.D. (2007). Dissociable intrinsic connectivity networks for salience processing and executive control. *J. Neurosci.* 27, 2349–2356.
- Shirer, W.R., Ryali, S., Rykhlevskaia, E., Menon, V., and Greicius, M.D. (2012). Decoding subject-driven cognitive states with whole-brain connectivity patterns. *Cereb. Cortex* 22, 158–165.
- Siebenhühner, F., Weiss, S.A., Coppola, R., Weinberger, D.R., and Bassett, D.S. (2013). Intra- and inter-frequency brain network structure in health and schizophrenia. *PLoS ONE* 8, e72351.
- Spadone, S., Della Penna, S., Sestieri, C., Betti, V., Tosoni, A., Perrucci, M.G., Romani, G.L., and Corbetta, M. (2015). Dynamic reorganization of human resting-state networks during visuospatial attention. *Proc. Natl. Acad. Sci. USA* 112, 8112–8117.
- Sporns, O. (2011). *Networks of the Brain* (Cambridge, Mass: MIT Press).
- Wang, Z., Liu, J., Zhong, N., Qin, Y., Zhou, H., and Li, K. (2012). Changes in the brain intrinsic organization in both on-task state and post-task resting state. *Neuroimage* 62, 394–407.
- Warren, D.E., Power, J.D., Bruss, J., Denburg, N.L., Waldron, E.J., Sun, H., Petersen, S.E., and Tranel, D. (2014). Network measures predict neuropsychological outcome after brain injury. *Proc. Natl. Acad. Sci. USA* 111, 14247–14252.
- Yeo, B.T., Krienen, F.M., Sepulcre, J., Sabuncu, M.R., Lashkari, D., Hollinshead, M., Roffman, J.L., Smoller, J.W., Zöllei, L., Polimeni, J.R., et al. (2011). The organization of the human cerebral cortex estimated by intrinsic functional connectivity. *J. Neurophysiol.* 106, 1125–1165.
- Zalesky, A., Fornito, A., Egan, G.F., Pantelis, C., and Bullmore, E.T. (2012). The relationship between regional and inter-regional functional connectivity deficits in schizophrenia. *Hum. Brain Mapp.* 33, 2535–2549.

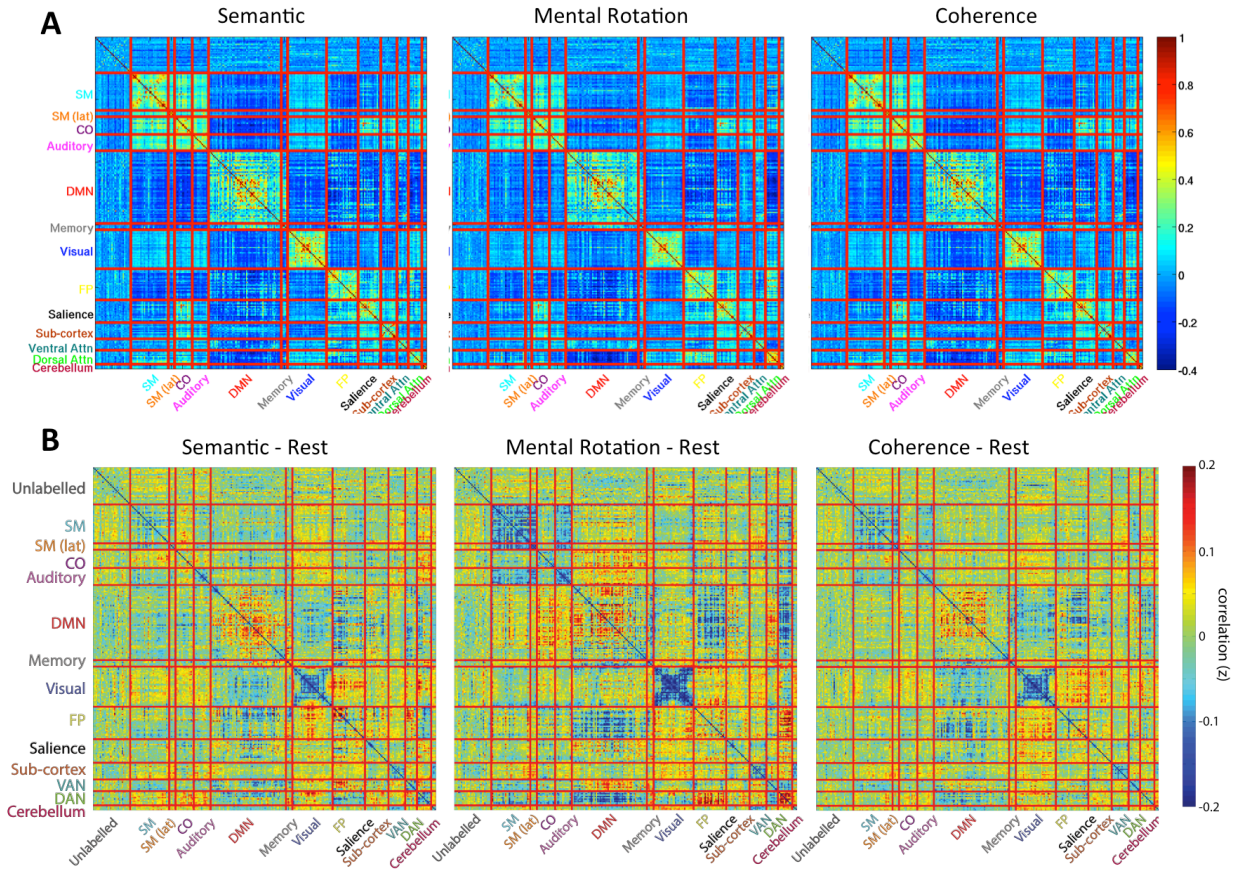
Cell Reports, Volume 17

Supplemental Information

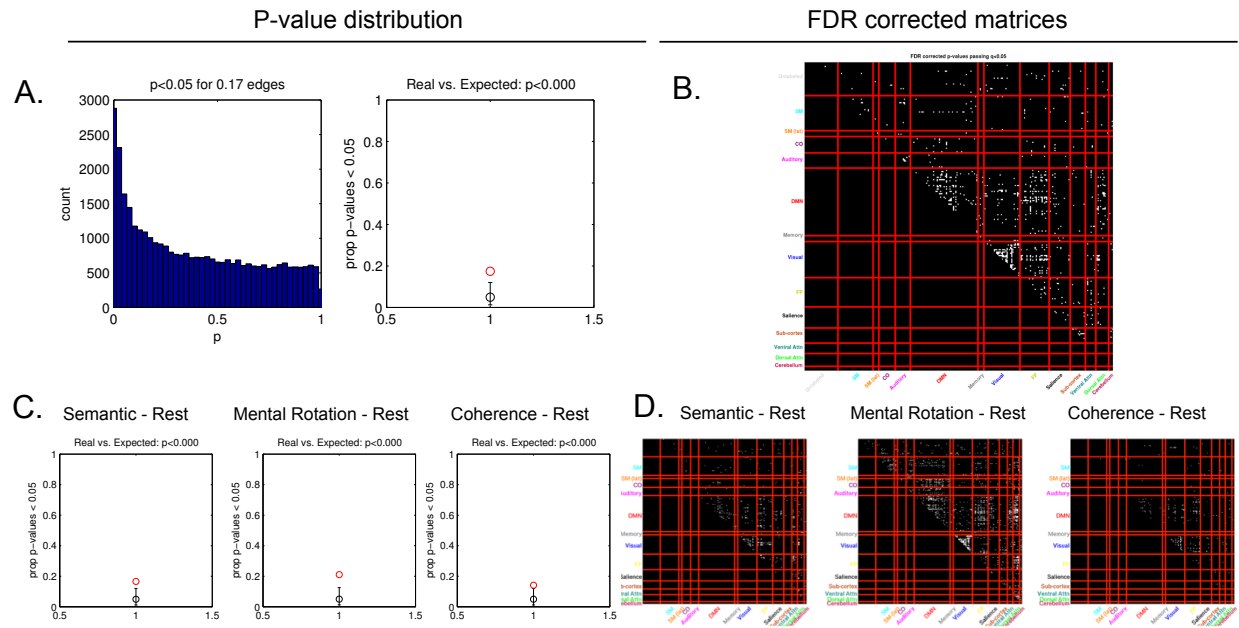
**Evidence for Two Independent Factors
that Modify Brain Networks to Meet Task Goals**

**Caterina Gratton, Timothy O. Laumann, Evan M. Gordon, Babatunde
Adeyemo, and Steven E. Petersen**

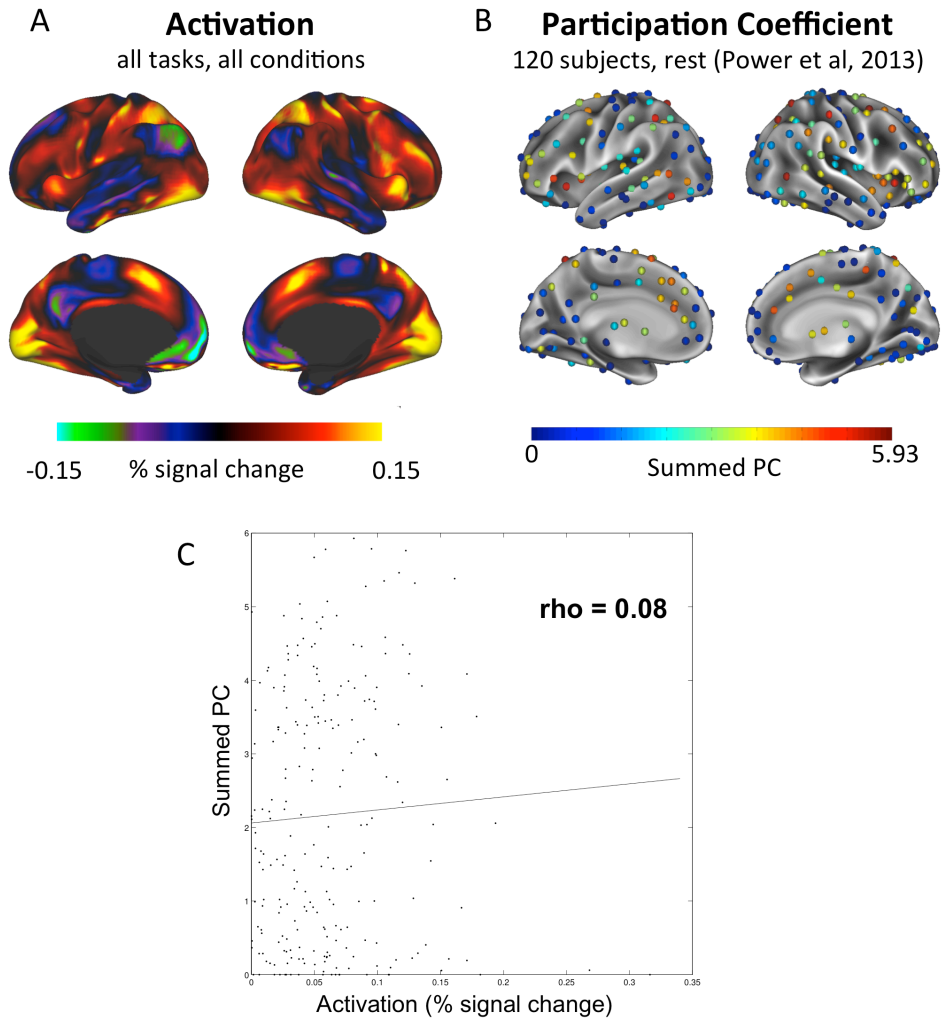
SUPPLEMENTARY FIGURES



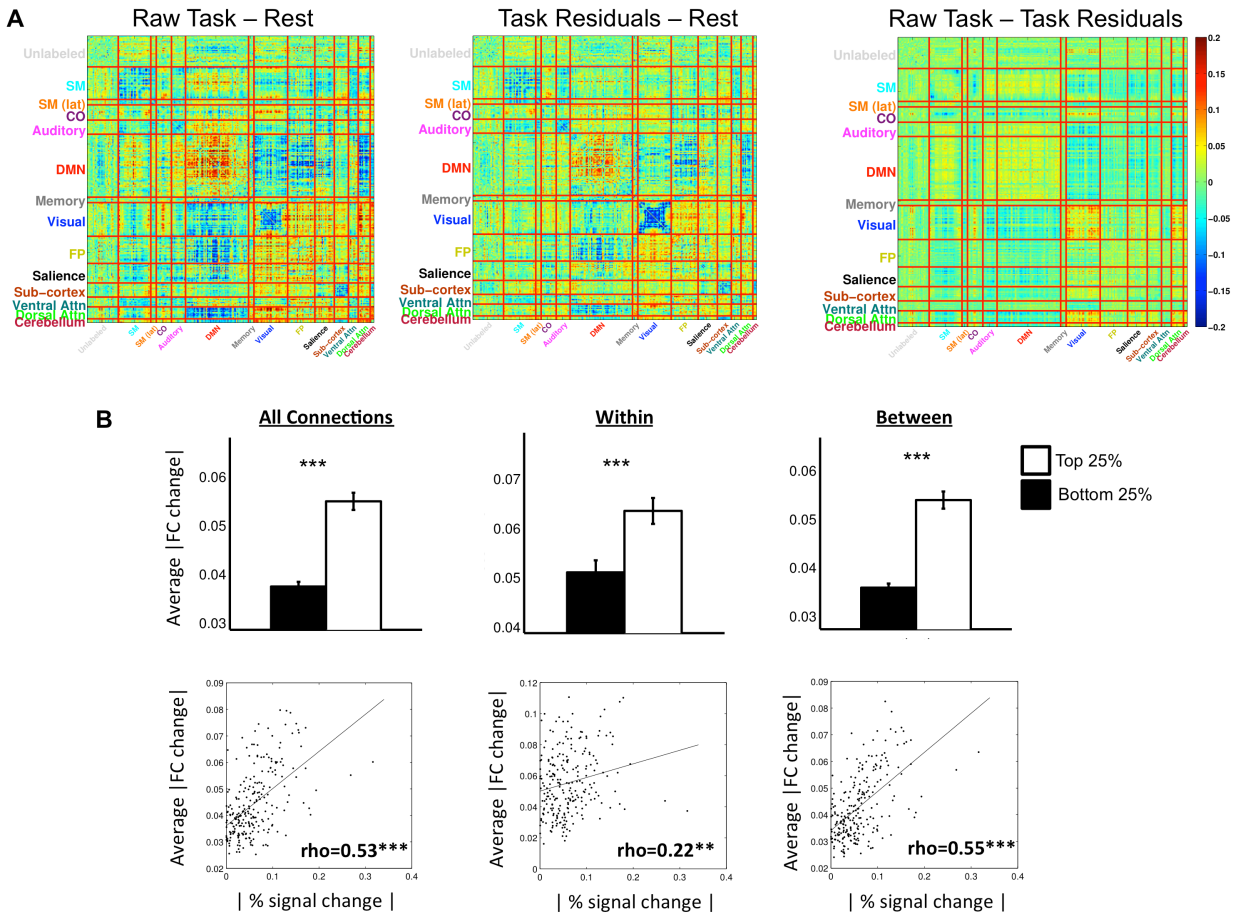
Supp. Figure 1: Correlation Matrices For Each Task, Related to Figs. 2-3. (A) Correlation matrices for 264 regions during the semantic (left), mental rotation (middle), or coherence (right) tasks. (B) Differences in FC were seen between each individual task and rest, many of which were shared across tasks (and seen in the all-task comparison of Figure 4). For example, the visual system showed decreased within and increased between network correlations, the default mode system showed increased within and decreased between network correlations..



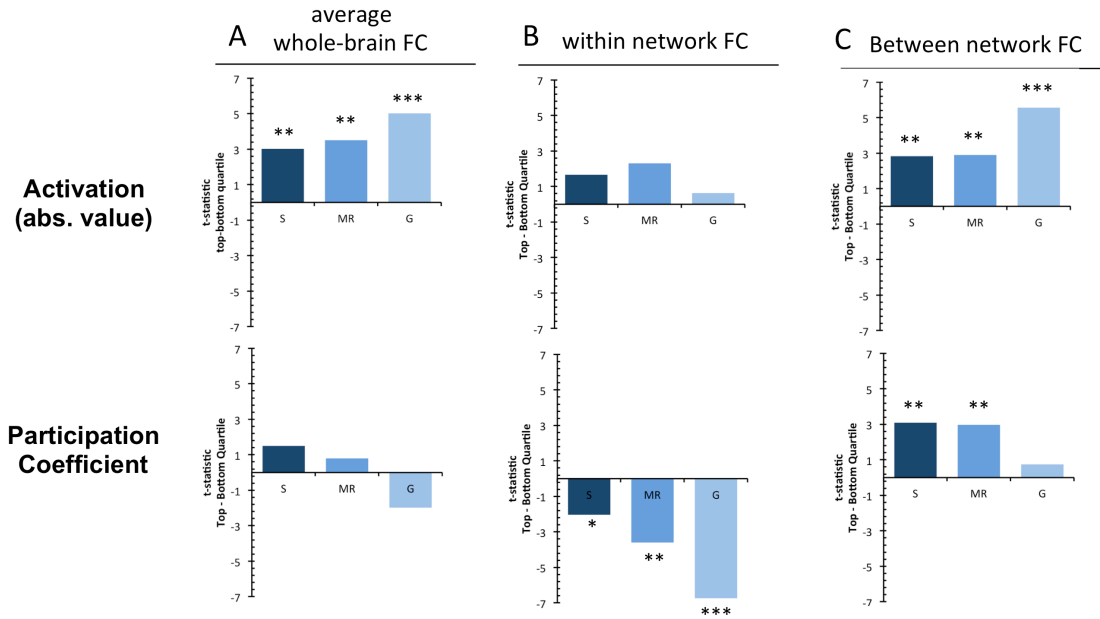
Supp. Figure 2: Statistical Quantification of the Differences Between Task and Rest FC, Related to Fig. 3. (A) The distribution of p-values comparing task and rest matrices is strongly skewed toward lower values, unlike randomized (permuted) comparisons ($p < 0.001$). (B) FDR correction ($q < 0.05$) shows many connections that pass multiple comparisons correction, despite the large number of comparisons. (C & D) Similar effects are seen when tasks are considered individually.



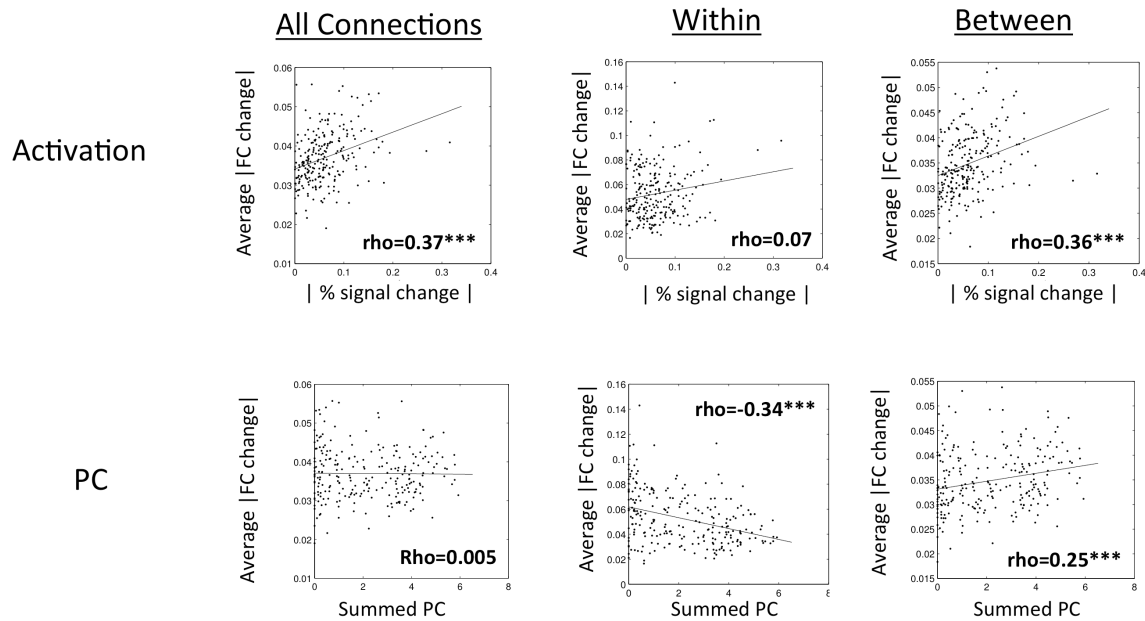
Supp. Figure 3: Activation and PC for Each Region, Related to Fig. 1&4. (A) The average activation (average percent signal change for all three tasks and conditions compared with baseline) for each voxel is displayed on a projected cortical surface. (B) The participation coefficient for each of 264 regions of interest was calculated in a sample of 120 individuals at rest (Power et al. 2013). These summed PC values are displayed here; warmer colors indicate connector-hub nodes. (C) Activation during our tasks was not correlated with participation coefficient (Spearman's $\rho = 0.08$, $p=0.23$). Each point on the plot represents a single region.



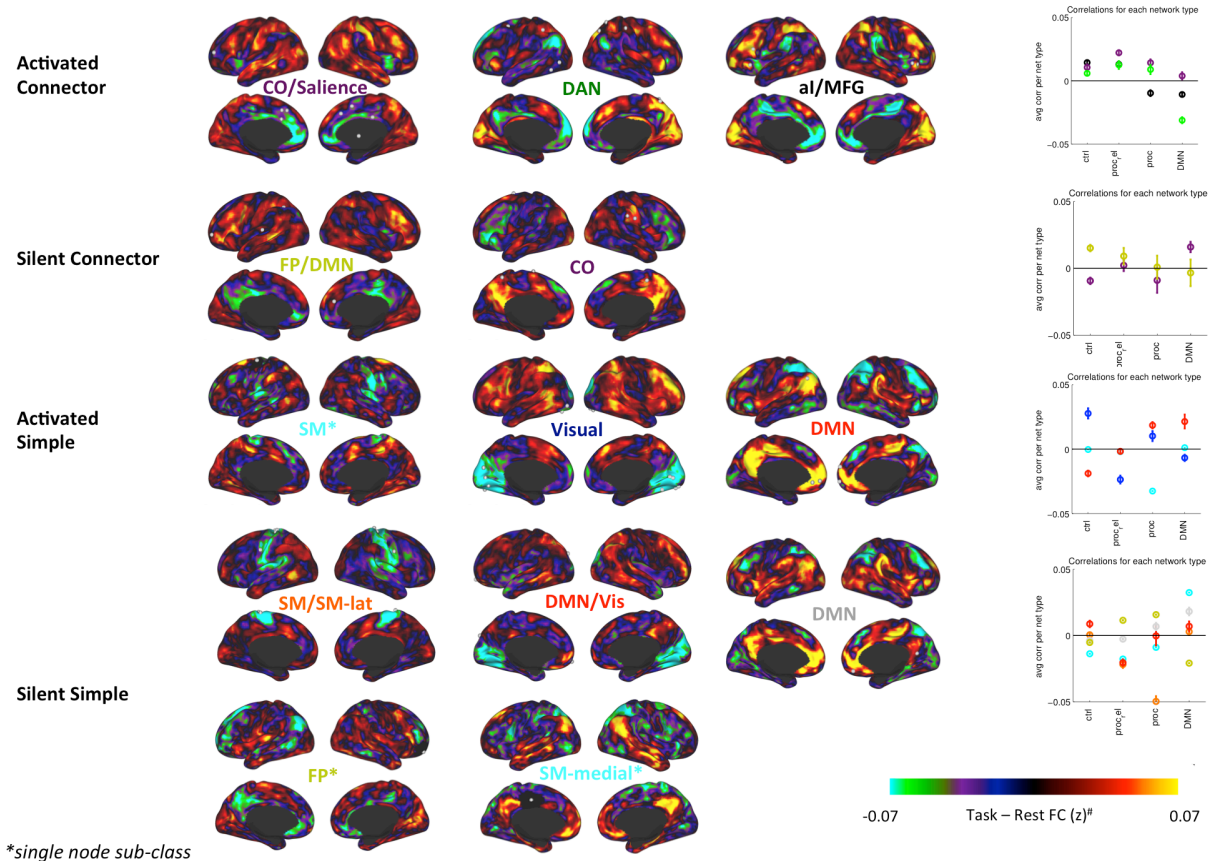
Supp. Figure 4: Comparison of Raw Task and Task Residuals, Related to Fig. 4, Supp. Fig. 6. (A) FC calculated with raw task data showed a very similar pattern of changes as FC calculated from the residuals of task processing (left and center) and only small quantitative differences (right). (B) However, as would be expected, using raw task data without the removal of evoked activation effects artificially increases the relationship between FC and activation for all effects (compare with Figure 4, Supp. Figure 6).



Supp. Figure 5: Quartile Analysis for Each Task, Related to Fig. 4. Quartile analysis of the mean changes in FC for different types of nodes for individual tasks (S = semantic, MR = mental rotation, G = coherence with Glass patterns), displayed as the t-statistic of the difference between top and bottom quartile nodes (p-values were computed using permutation tests and FDR corrected for multiple comparisons across tasks; * $p < 0.05$, ** $p < 0.01$, *** $p < 0.001$). (A) FC changes more for highly activated nodes than non-activated nodes (top) in all three tasks, but there is no consistent difference between high and low PC nodes across tasks. (B) Within network connections were numerically but not significantly higher for activated nodes than non-activated nodes (top). High PC nodes showed significantly more stable within-network FC with respect to low PC nodes in all tasks (bottom). (C) Between network connectivity was significantly altered in 3/3 tasks for high activation regions (top) and 2/3 tasks for high PC regions (bottom).



Supp. Figure 6: Correlations between Activation/PC and FC Changes, Related to Fig. 4, Supp. Table 1&3. An alternative approach was used to examine the relationship between activation/PC and changes in FC, using Spearman correlations (thereby treating these variables as continuous measures). We found similar relationships: a moderate positive relationship between activation and FC for all connections (top left) and between network connections (top right), and a small relationship with within network connections. We also found a significant positive relationship between PC and FC for between network connections (bottom right), with a significant negative relationship with within network connections (bottom middle), with no relationship for connections on average (bottom left). Individual points in the scatter plots show single nodes. FC changes were based on the mean absolute difference in task and rest FC, activation was defined as the absolute percent signal change of a region, and PC was defined as the summed PC value across thresholds. Spearman's correlation values for individual tasks are reported in Supp. Table 1.



Supp. Figure 7: Topography of FC changes for Each Class, Related to Fig. 6. Within each class, nodes differed in the specific topography of FC changes. Here, we represent the predominant patterns (or sub-classes) exhibited by each class. Sub-classes were identified via data-driven hierarchical clustering of the FC maps. The activated connector class showed 3 sub-classes, associated primarily with nodes in the CO/Saliency network, the DAN, and the anterior insula/L middle frontal gyrus, respectively. These nodes tended to show increased FC across control systems and relevant processing systems (i.e., visual, dorsal somatomotor), but decreased connectivity with regions in the default mode network. The silent connector system exhibited two main patterns of changes. The FP/DMN group showed increased connectivity mostly across control systems. The CO group showed decreased connectivity with control systems and increased connectivity with the default mode. The activated simple class showed three main patterns: a visual sub-class which exhibited decreased connectivity with visual regions and increased connectivity with control systems, a default mode network sub-class which showed increased connectivity to default mode regions and decreased connectivity to control systems, and a single somatomotor node which primarily showed decreased connectivity with other somatomotor regions. The predominant pattern of the silent simple class was decreased connectivity; nodes did not group well into sub-classes (besides a single somatomotor sub-class, all the rest had 1 or 2 nodes only). Two of these subclasses (DMN and SM-medial) showed some increases in connectivity with DMN regions. The typical changes seen for each sub-class are quantified in the plot to the right of each row, with colored dots representing the average change in FC for a set of sub-class of seeds to a target set of networks (as in Fig. 6). #: Note that FC calculations excluded correlations within 20mm of a seed node.

SUPPLEMENTARY TABLES

Individual Task Spearman's rho	Semantic	Mental Rotation	Coherence
Activation			
All FC	0.20**	0.21**	0.28***
Within FC	0.11	0.11	-0.02
Between FC	0.17*	0.17*	0.33***
PC			
All FC	0.15~	0.02	-0.10
Within FC	-0.12~	-0.26***	-0.40***
Between FC	0.27***	0.22**	0.08

~p<0.10, *p<0.05, **p<0.01, ***p<0.001, FDR corrected

Supp. Table 1: Correlations between Activation/PC and FC for Each Task, Related to Fig. 4, Supp. Figs. 5&6. Spearman's correlations between changes in FC and activation (top set) or PC (bottom set) for each individual task. Results were similar across tasks. Activation was related to overall FC changes and between-network FC changes for all 3 tasks. PC was negatively related to within-network FC changes and positively related to between-network FC changes for 2/3 tasks (and numerically in the same direction in the third task; *p-values FDR corrected for multiple comparisons*).

Bin thresholds	10%	25%	33%
Activation			
All FC	***	***	***
Within FC	~	n.s.	n.s.
Between FC	**	***	***
PC			
All FC	~	n.s.	n.s.
Within FC	**	***	***
Between FC	***	**	**

~ p<0.10, *p<0.05, **p<0.01, ***p<0.001

Supp. Table 2: Binned Analyses with Different Bin Thresholds, Related to Fig. 4. Quartile analysis results contrasting FC changes for top and bottom activated regions (top-set) or high and low PC regions (bottom-set) were unchanged if other binning thresholds were used.

	Full Model R ²	Full Model F(1,232)	PC t(235)	Activation t(235)	PC * Activation t(235)
whole-brain FC	0.122	10.8***	-0.529	5.23***	-0.648
within-network FC	0.166	15.4***	-5.781***	2.64**	-1.174
between-network FC	0.143	12.9***	3.190**	4.958***	0.09

Supp. Table 3: Linear Regression Model, Related to Figure 4. Linear regression model explaining average absolute changes in connectivity across all connections (*top row*), within network connections (*middle row*) or between network connections (*bottom row*). The model included regressors for PC, activation, and their interaction. *** $p < 0.001$, ** $p < 0.01$

SUPPLEMENTARY EXPERIMENTAL PROCEDURES

Behavioral Paradigms and Stimuli

Detailed information regarding the three tasks is reported in Dubis et al. (2014); we briefly summarize relevant parameters here. Three runs for each task were completed in a session in counterbalanced order. Each run was 7.7 min long. Runs consisted of two task blocks, each flanked by 50s (20 frames) of fixation. Each task had a mixed block/event-related design. Task blocks were initialized with a 1000ms start cue. The fixation cross changed color to mark the start of the task and the display indicated which button corresponded to each response category (i.e., “noun” vs. “verb” for the semantic task, “mirror” vs. “same” for the mental rotation task, or “coherence” vs. “no coherence” for the coherence task). Response hand was counterbalanced by task. The start cue was followed by individual trials in each task. Each trial lasted a single 2.5s frame. In a task block, 30 trials were mixed with 32 null events and jittered with a uniform distribution of 0-2 frames between subsequent trials. Stimuli were presented for 500ms. At the end of the block, a 1000ms end cue appeared consisting of a color change in the fixation cross.

Semantic Task: In the semantic task, participants were asked to complete a noun/verb judgment on verbal stimuli. Stimuli consisted of common 6-letter nouns (90) and verbs (90); 15 nouns and 15 verbs were presented in a single block. Words were presented in white 48pt Helvetica font on a black background.

Mental Rotation Task: In the mental rotation task, two shapes were presented on either side of the fixation cross. Participants were asked to determine whether the stimuli were the same shape, but rotated with respect to one another, or mirror images. The stimuli consisted of one of 8 white 2D shapes composed of 7 squares on a black background. Three rotation orientation bins were used: 40-60°, 100-120°, and 150-170°.

Coherence Task: In the coherence task, concentric Glass patterns (Glass, 1969), consisting of white dots on a black background, were presented. In the patterns, dot pairs could either be coherently aligned in a circular pattern or randomly dispersed. Four bins of coherence were used: 0%, 12.5% (typical perceptual threshold level [Wilson 1997]), 25%, and 50%. Participants were asked to determine whether dots were coherently arranged or not. Dots were 1 pixel large (0.04° if visual angle) and presented with a density of 88 dot pairs/degree².

Data Preprocessing:

All data was first processed using steps to reduce artifacts in the data (Miezin et al., 2000). These steps included (a) application of a rigid body algorithm to correct for motion within and across runs (Snyder, 1996), (b) intensity normalization to a mode of 1000 across the whole brain to allow for inter-subject comparisons (Ojemann et al., 1997), (c) temporal realignment of slices to midpoint of first slice using sinc-interpolation to account for slice acquisition time, and (d) resampling to 3mm isotropic space and (e) transformation to a stereotaxic atlas (Talairach and Tournoux, 1988). During atlas registration, a subject’s anatomical image was aligned with a custom atlas-transformed (Lancaster et al., 1995) target template using a series of affine transforms (Snyder, 1996). All spatial transforms are composed for one-step resampling from native to atlas space using cubic spline interpolation.

FC Processing Details:

A series of processing steps was applied to both task and resting-state time series with the aim of reducing artifacts in FC analysis as in Power et al. (2014). FC Processing was done in two iterations. In the first pass, data was minimally processed (demean, detrend, filtering; see below) for quality control and motion contaminated volumes (framewise displacement > 0.2; (Power et al., 2012)) were identified. All volumes with motion and 15 frames from the start and end of runs (to reduce filter artifacts) were marked for removal. In addition, any remaining segments of the data that were less than 5 contiguous frames long were marked. The marked frames were used to create temporal masks of censored data. Participants with fewer than 120 remaining frames were excluded from analysis (1 all-task, and 4 single-task participants). Only participants with both resting state and task data were analyzed in any given comparison. This left 28 participants in rest vs. all-task analyses and 25 participants in rest vs. single-task analyses. On average, 762 resting state (148 – 2809, 65% on average), 961 (291-1232, 79%) all-task, and 340 (183-414, 81%) single-task volumes were retained in remaining participants.

In the second pass of FC processing (1) data was demeaned and detrended, (2) nuisance variables were regressed from the data, including whole brain, cerebrospinal fluid, and white matter signals, as well as signals from a Volterra expansion of motion parameters (Friston et al., 1996), and (3) a bandpass filter (0.009 – 0.08 Hz) was applied to the data. Notably, data from the censoring mask was ignored in the regression step, and after regression, data was

interpolated across censored frames using least squares spectral estimation (Power et al., 2014) to avoid contaminating nearby frames during bandpass filtering (Carp, 2013). In addition, (4) spatial smoothing (6mm) was applied to the dataset after filtering. As a final step, (5) censored frames were removed from the time series

Participation coefficient (PC): PC is a measure of the distribution of connections across networks (Guimera and Amaral, 2005):

$$P_i = 1 - \sum_{s=1}^{N_M} \left(\frac{k_{is}}{k_i} \right)^2$$

where the i is a node, k_{is} is the number of connections between node i to nodes in module s , and k_i is the degree for node i .

Regions with high PC are termed *connector hubs*. To have a robust estimate of PC for each brain region, we used PC values computed from a set of 120 individuals at rest across a range of graph thresholds, and then summed across thresholds to produce a final “summed PC” value (Power et al., 2013). Although Guimera and Amaral (2005) identified 7 distinct functional roles for nodes based on PC and within module degree, these 7 classes are not easily identifiable in FC-MRI brain networks (Power et al., 2013). We consequently focused on PC given its connection with disruptions after brain lesions (Gratton et al., 2012; Warren et al., 2014).

Measuring Topography of Classes: We computed whole-brain seedmaps for every ROI in a class during task and rest (excluding voxels within 20mm of a given seed for this and all following analyses to reduce the influence of local signal spread). Differences in the topography between seedmaps were quantified via the average task-rest FC difference for a given node to voxels in each network. We report network averages grouped by the type of network (i.e., control network, processing network, etc.). Unlike magnitude analyses, no absolute value was taken. Analyses were done across ROIs and FDR corrected two-sample t-tests (corrected across network types) were used to determine significance. Detailed patterns of FC changes for subsets of nodes are shown in Supp. Fig. 6 (see *Measuring topographic patterns in sub-classes of regions* below).

Measuring topographic patterns in sub-classes of regions (Supp. Fig. 7): Since individual nodes showed unique specific patterns of FC changes, even within a class, we used data-driven hierarchical clustering to identify sub-classes of nodes that showed similar patterns of FC changes (see **Hierarchical Clustering** below for details). Then, the topographic distribution of FC changes was quantified by averaging the FC task-rest difference for any given node to voxels in each network (Power et al., 2011) (voxels within 20mm of a seed were excluded from analysis to avoid biasing estimates by spatial autocorrelation). These were then averaged for each type of network (*control = CO, Salience, FP, DAN, VAN; relevant processing = visual, SM; processing = SMlat, auditory; DMN = DMN*).

Hierarchical Clustering: Hierarchical clustering was used to identify sets of regions that showed similar changes in connectivity between task and rest within each class. In addition, hierarchical clustering was used to examine the relationship between activated and silent connector regions in the CO network. For this analysis, seed connectivity analyses were conducted on previously identified regions of interest (e.g., “activated connectors”), where the correlation was taken between a spherical ROI seed and every other brain voxel. A difference seed-map was created by subtracting the rest seed map from the all-task seed-map. These difference seed-maps were then submitted to a clustering analysis. In the clustering analysis, the distance between correlation maps was computed by taking a “1 - r” calculation, where “r” represents the correlation between difference maps from different regions. Regions within 20 mm of each seed were excluded from analysis. The distances were then entered into a UPGMA (unweighted paired group method with arithmetic mean (Handl et al., 2005)) hierarchical clustering algorithm in Matlab R2012a (7.14, [The Mathworks; Natick, MA]). In this algorithm, clusters are progressively united at each step based on the average distance between all points in a cluster (this approach is thought to produce relatively robust, unbiased estimates compared with other hierarchical clustering algorithms (Eisen et al., 1998; Ploran et al., 2007)). A separate modularity analysis (Newman, 2006) of the linkages was used as an objective method to determine where to cut the dendrogram (i.e., the number of clusters present in the data at maximal modularity).

Flexibility across tasks: We predicted that regions involved in task control should change their configurations in different tasks. Therefore, we measured how flexible, or variable, nodes were in their FC topography across tasks by correlating the FC task-rest difference seedmap of each node between the three tasks. We then averaged the (Fisher-transformed) correlation values across task comparisons. Low correlations, or more across-task variability, were

taken to be indicative of flexibility. Flexibility was compared between classes using two-sample t-tests, FDR correcting for multiple comparisons between classes.

Activated vs. silent connectors in CO: We compared FC topography for activated and silent connectors that were part of the CO network (defined as CO based on the voxelwise networks from Power 2011). The comparison included (a) hierarchical clustering of the task-rest difference seedmaps from all activated and silent connector CO regions (see *Hierarchical Clustering*, above; the dendrogram was cut to produce two clusters), (b) two-tailed two-sample t-tests of the FC difference seedmap for activated vs. silent connectors (thresholded at $p < 0.001$ uncorrected for visualization purposes only) and (c) average FC difference for activated and silent connectors to voxels in each network, sorted by network type (as above; FDR corrected for multiple comparisons across network types).

References

- Carp, J. (2013). Optimizing the order of operations for movement scrubbing: Comment on Power et al. *NeuroImage* 76, 436-438.
- Eisen, M.B., Spellman, P.T., Brown, P.O., and Botstein, D. (1998). Cluster analysis and display of genome-wide expression patterns. *Proceedings of the National Academy of Sciences of the United States of America* 95, 14863-14868.
- Friston, K.J., Williams, S., Howard, R., Frackowiak, R.S., and Turner, R. (1996). Movement-related effects in fMRI time-series. *Magnetic resonance in medicine* 35, 346-355.
- Glass, L. (1969). Moire effect from random dots. *Nature* 223, 578-580.
- Gratton, C., Nomura, E.M., Perez, F., and D'Esposito, M. (2012). Focal brain lesions to critical locations cause widespread disruption of the modular organization of the brain. *Journal of cognitive neuroscience* 24, 1275-1285.
- Guimera, R., and Amaral, L.A. (2005). Cartography of complex networks: modules and universal roles. *J Stat Mech* 2005, nihpa35573.
- Handl, J., Knowles, J., and Kell, D.B. (2005). Computational cluster validation in post-genomic data analysis. *Bioinformatics* 21, 3201-3212.
- Lancaster, J.L., Glass, T.G., Lankipalli, B.R., Downs, H., Mayberg, H., and Fox, P.T. (1995). A modality-independent approach to spatial normalization of tomographic images of the human brain. *Human brain mapping* 3, 209-223.
- Newman, M.E. (2006). Modularity and community structure in networks. *Proceedings of the National Academy of Sciences of the United States of America* 103, 8577-8582.
- Ojemann, J.G., Akbudak, E., Snyder, A.Z., McKinstry, R.C., Raichle, M.E., and Conturo, T.E. (1997). Anatomic localization and quantitative analysis of gradient refocused echo-planar fMRI susceptibility artifacts. *NeuroImage* 6, 156-167.
- Ploran, E.J., Nelson, S.M., Velanova, K., Donaldson, D.I., Petersen, S.E., and Wheeler, M.E. (2007). Evidence accumulation and the moment of recognition: Dissociating perceptual recognition processes using fMRI. *The Journal of neuroscience : the official journal of the Society for Neuroscience* 27, 11912-11924.
- Power, J.D., Barnes, K.A., Snyder, A.Z., Schlaggar, B.L., and Petersen, S.E. (2012). Spurious but systematic correlations in functional connectivity MRI networks arise from subject motion. *Neuroimage* 59, 2142-2154.
- Power, J.D., Schlaggar, B.L., Lessov-Schlaggar, C.N., and Petersen, S.E. (2013). Evidence for hubs in human functional brain networks. *Neuron* 79, 798-813.
- Snyder, A.Z. (1996). Difference image vs. ratio image error function forms in PET-PET realignment. In *Quantification of Brain Function Using PET*, R. Myer, V.J. Cunningham, D.L. Bailey, and T. Jones, eds. (San Diego, CA: Academic Press), pp. 131-137.
- Talairach, J., and Tournoux, P. (1988). *Co-Planar Stereotaxic Atlas of the Human Brain* (New York: Thieme Medical Publishers, Inc.).
- Warren, D.E., Power, J.D., Bruss, J., Denburg, N.L., Waldron, E.J., Sun, H., Petersen, S.E., and Tranel, D. (2014). Network measures predict neuropsychological outcome after brain injury. *Proceedings of the National Academy of Sciences of the United States of America* 111, 14247-14252.